MAGNETIC FIELD MEASUREMENT METHODS

Carl Heiles, UC Berkeley

HOW WE MEASURE MAGNETIC FIELDS:

Bpar (line-of-sight component of field strength)

> Faraday rotation, depolarization, "Faraday synthesis"

> Zeeman splitting, including radiative transfer effects

Bperp (orientation on plane of sky):

> polarization of absorbed background light by aligned dust

> polarization of emitted IR by aligned dust

> Chandrasekhar-Fermi method

> Goldreich-Kylafis (a.k.a. Hanle?) effect

> polarization position angle of Synchrotron emission

Btot (total field strength)

> Zeeman splitting, with [splitting > linewidth], some masers

> Synchrotron emissivity (with assumptions)

> Direct dynamical effects (Houde et al.)

Bpar:

Faraday rotation

Faraday rotation is the rotation of the position angle of a linearly polarized wave as it propagates.

The two equal-amplitude circular polarizations with relative phase φ produce linear polarization, with position angle equal to φ/2.

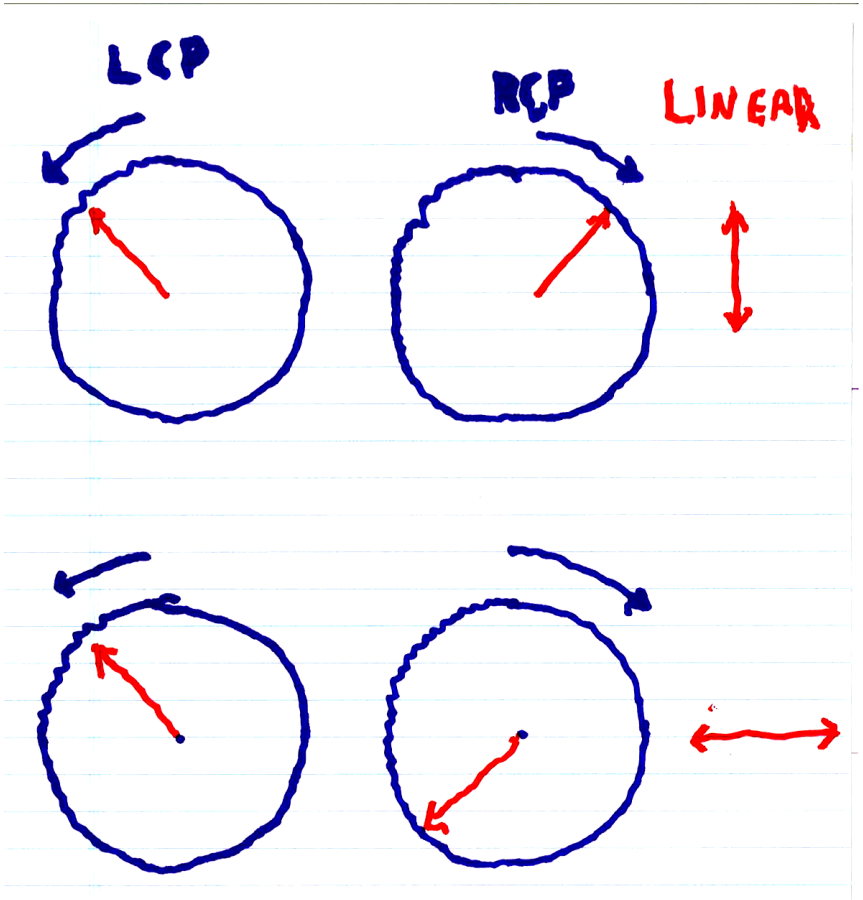

1. FARADAY ROTATION

The phase velocity v_{ph} is

$$\left(\frac{v_{ph}}{c}\right)^2 = \left[1 - \frac{\nu_p^2}{\nu\left(\nu \pm \nu_c \cos(\theta)\right)}\right]^{-1}$$

where the $\pm$ applies to LCP or RCP, and θ is the angle of the B field to the line of sight.

$\nu_c = \frac{eB}{2\pi m_e c} = 2.8 B_{\mu G}$ **Hz** is the cyclotron frequency

$\nu_p = \left(\frac{n_e c^2}{\pi m_e}\right)^{1/2} = 9.0 n_e^{1/2}$ **kHz** is the plasma frequency

Because $\nu_c \ll \nu_p \ll \nu$, let's Taylor-expand:

$$\frac{v_{ph}}{c} = 1 + \underbrace{\frac{1}{2}\left(\frac{\nu_p}{\nu}\right)^2}_{(pulsar\ dispersion)} \mp \underbrace{\frac{1}{2}\left(\frac{\nu_p}{\nu}\right)^2\left(\frac{\nu_c}{\nu}\right)\cos(\theta)}_{(Faraday\ rotation)}$$

Two circulars of equal amplitude combine to produce linear. The position angle depends on the relative phase $\phi/2$.

As the wave propagates over distance L, the RCP is delayed in time relative to the LCP by

$$\Delta t = \left(\frac{L}{v_{ph,RCP}}\right) - \left(\frac{L}{v_{ph,LCP}}\right) \approx L\frac{\Delta v_{ph}}{c^2}$$

The phase difference $\Delta\phi = \nu\Delta t$, so

$$\frac{\Delta\phi}{\Delta L} = \frac{\nu_p^2\nu_c}{c\nu^2}\cos(\theta) = RM\ \lambda^2$$

With all the constants, the Faraday Rotation Measure RM is

$$RM = 0.81\int\left(\frac{n_e}{\mathrm{cm}^{-3}}\right)\left(\frac{B_{||}}{\mu G}\right)dL_{pc}\ \mathrm{rad\ m}^{-2}$$

$B_{||}$ is the *line of sight* component of the magnetic field. *Positive* $B_{||}$ (points *away from* observer) gives *Negative* RM.

A similar analysis gives the Dispersion Measure DM

$$DM = \int \left(\frac{n_e}{\mathrm{cm}^{-3}}\right) dL_{pc}\ \mathrm{cm}^{-3}\mathrm{pc}$$

The final related quantity is the Emission Measure EM, directly proportional to the Hα line intensity and also the radio continuum and/or recombination line intensity

$$EM = \int \left(\frac{n_e^2}{\mathrm{cm}^{-6}}\right) dL_{pc}\ \mathrm{cm}^{-6}\mathrm{pc}$$

These quantities are often combined as if integral signs are simply algebraic symbols:

$$\left(\frac{B_{||}}{\mu G}\right) = \frac{\int \left(\frac{n_e}{\mathrm{cm}^{-3}}\right) \left(\frac{B_{||}}{\mu G}\right) dL_{pc}}{\int \left(\frac{n_e}{\mathrm{cm}^{-3}}\right) dL_{pc}} = \frac{RM}{0.81\, DM}$$

TAKE SUCH DERIVED VALUES WITH A GRAIN OF SALT!! They neglect correlations between n_e and B, which are *quite likely to occur*.

Example: the Crab Pulsar has $DM = 56.791$ cm^{-3} pc and $RM = -42.3$ rad m^{-2} (both are measured to *much* higher precision). At the 21 cm line, the position angle of linear polarization rotates 1.5 radians (86°!) and the pulse isdelayed by about 110 millisec (that's more than 3 pulsar periods!), both relative to infinite frequency. Our misleading equation gives $B_{||} \sim +0.9$ μG. *Note: The sign of* $B_{||}$ *is opposite the sign of* RM*. Also, positive fields point away from us.*

Systematic bias in interstellar magnetic field estimates

Rainer Beck[1], Anvar Shukurov[1,2], Dmitry Sokoloff[3], and Richard Wielebinski[1]

[1] Max-Planck-Institut für Radioastronomie, Auf dem Hügel 69, D-53121 Bonn, Germany
[2] School of Mathematics and Statistics, University of Newcastle, Newcastle upon Tyne, NE1 7RU, UK
[3] Department of Physics, Moscow State University, 119992 Moscow, Russia

Received 6 March 2003 / Accepted 1 July 2003

Abstract. Faraday rotation of the polarization plane in magnetized thermal plasma provides one of the most efficient methods to deduce regular magnetic fields from radio astronomical observations. Since the Faraday rotation measure RM is proportional to an integral, along the line of sight, of magnetic field weighted with thermal electron density, RM is believed to yield the regular magnetic field averaged over large volume. Here we show that this is not the case in a turbulent medium where fluctuations in magnetic field and electron density are not statistically independent, and so contribute to RM. For example, in the case of pressure equilibrium, magnetic field can be anticorrelated with plasma density to produce a negative contribution. As a result, the strength of the regular magnetic field obtained from RM can be *underestimated* if the fluctuations in electron density and magnetic field are neglected. The anticorrelation also reduces the standard deviation of RM. We further discuss the effect of the positive correlations where the standard treatment of RM leads to an *overestimated* magnetic field. Because of the anisotropy of the turbulent magnetic field, the regular magnetic fields strength, obtained from synchrotron emission using standard formulae, can be *overestimated*. A positive correlation between cosmic-ray number density and magnetic field leads to an overestimate of the strengths of the regular and total fields. These effects can explain the difference between the strengths of the regular Galactic magnetic field as indicated by RM and synchrotron emissivity data and reconcile the magnetic field strength in the Solar vicinity with typical strength of regular magnetic fields in external galaxies.

Price: Magnetic nature LOVES a vacuum!

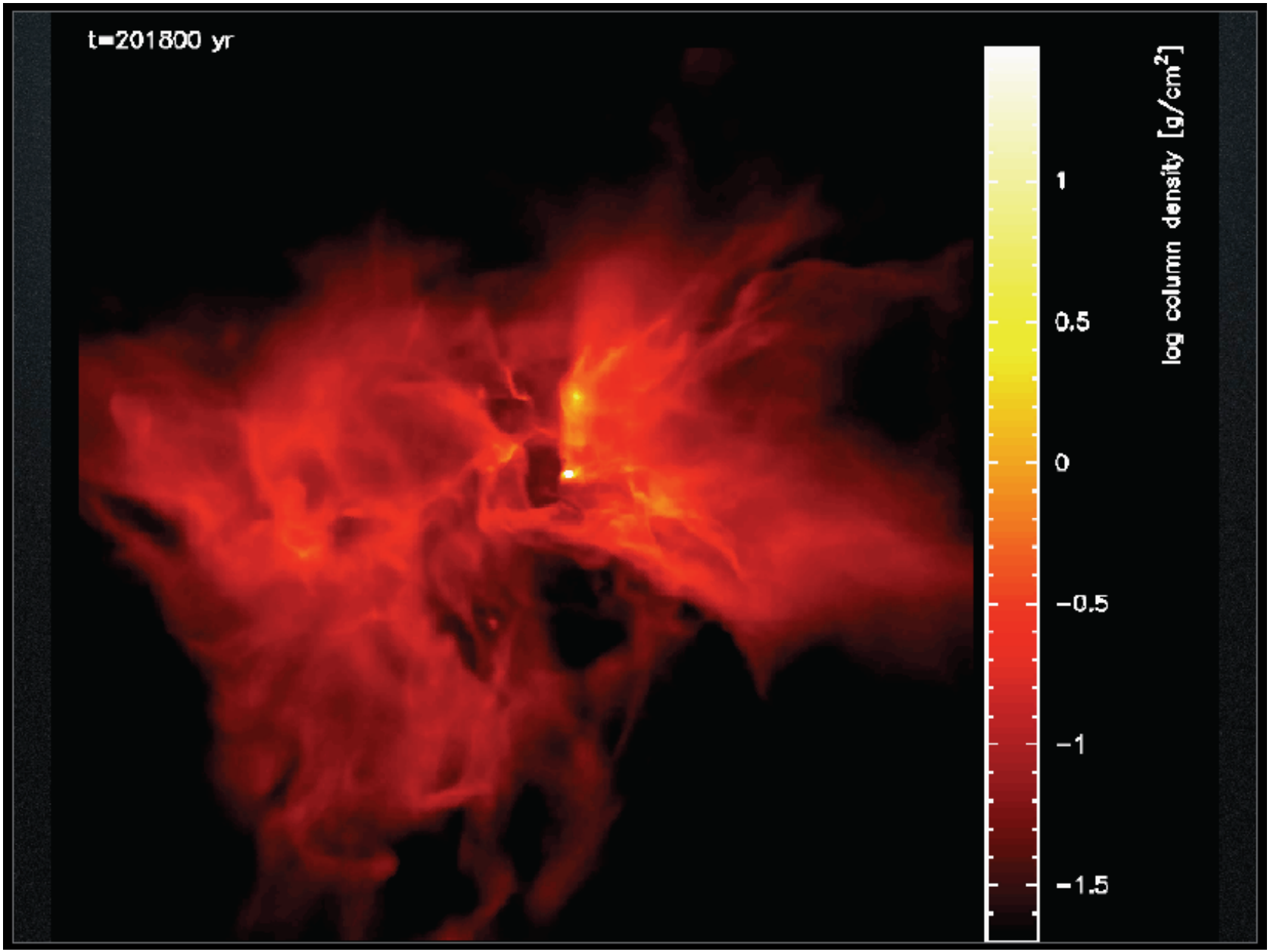

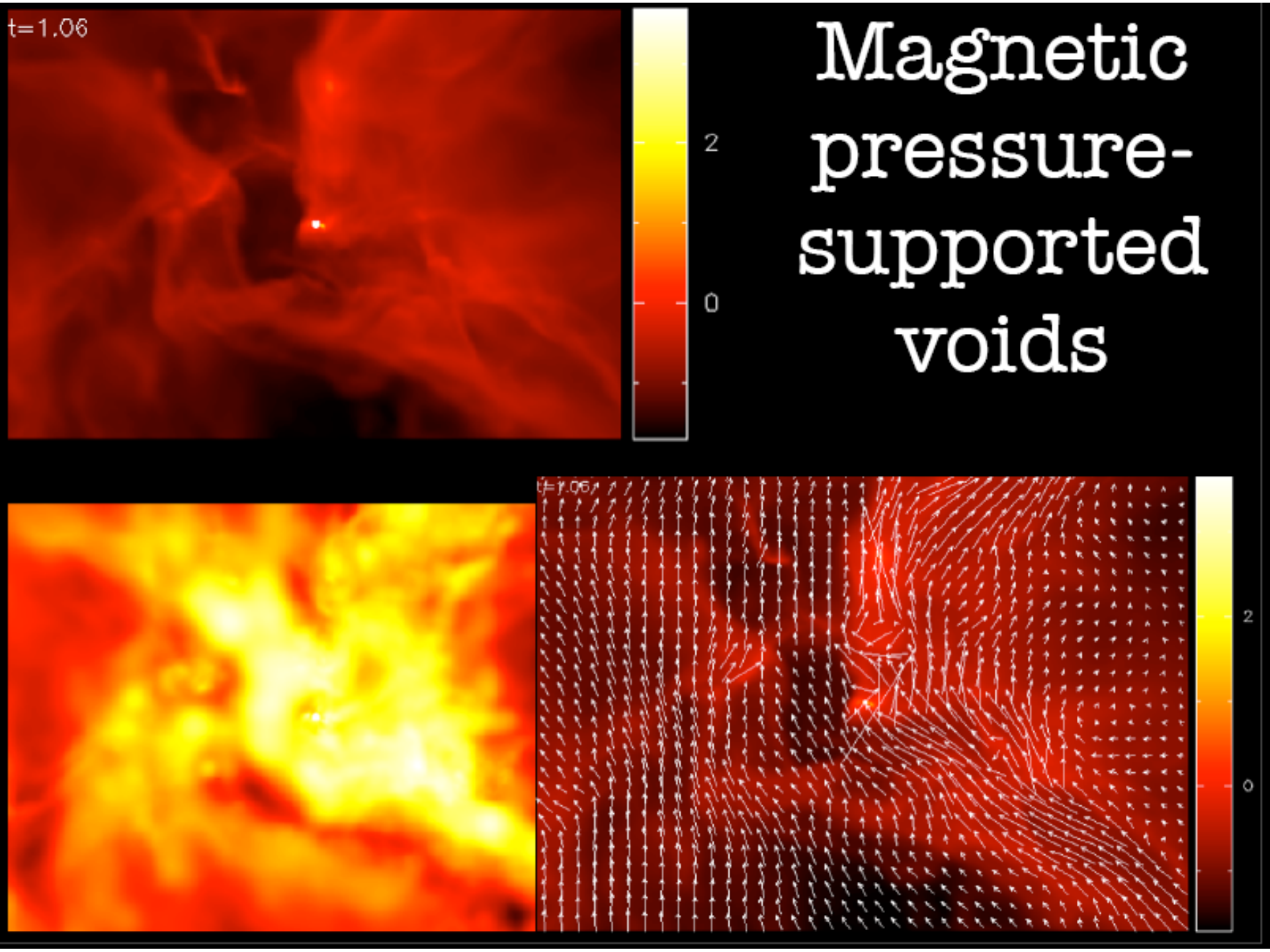
t=1.06
2
0
Magnetic pressure-supported voids
t=1.06
2
0


"stripiness"
Which MHD regime is most realistic?
beta > 1
beta < 1

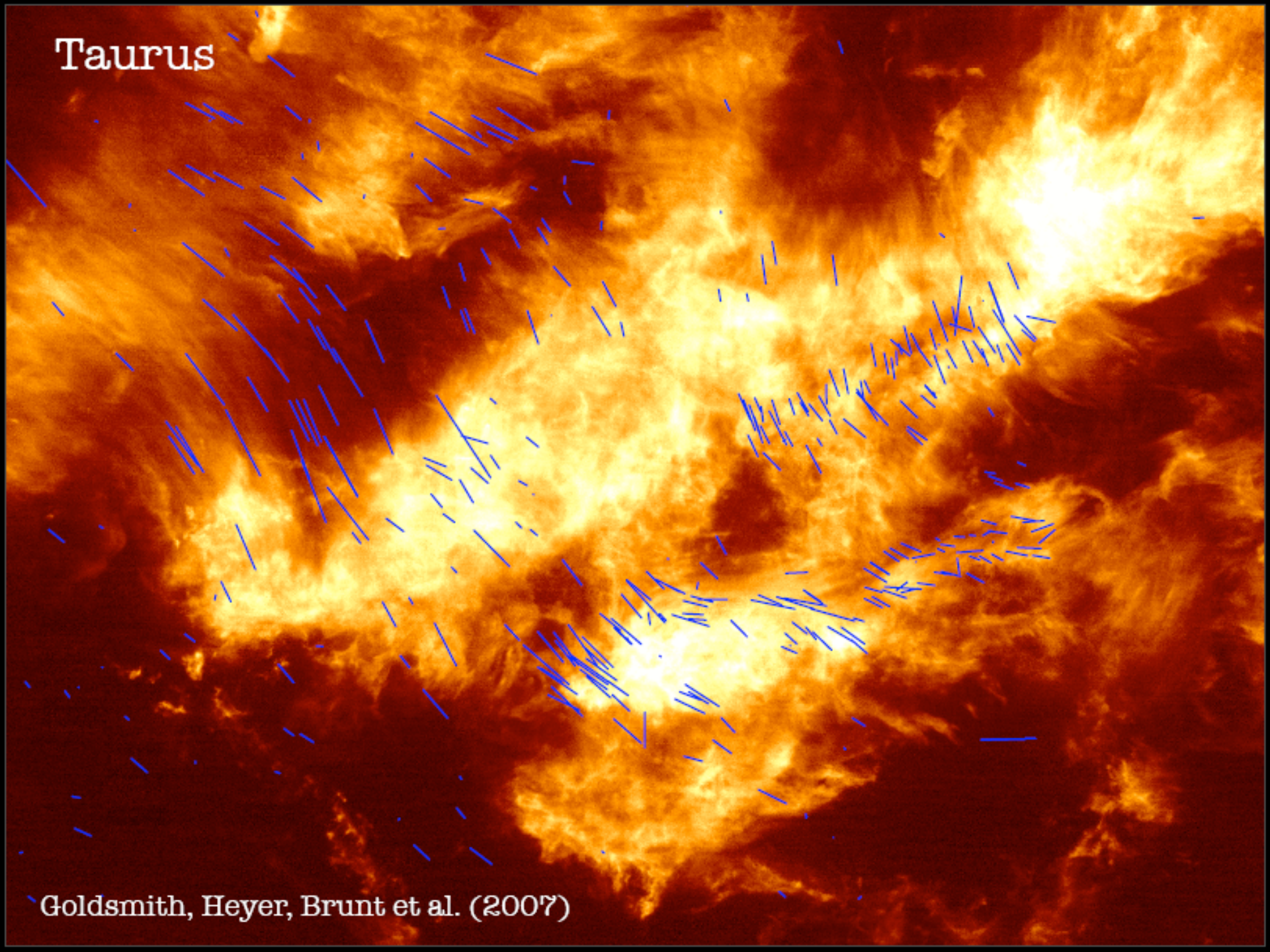
Taurus
Goldsmith, Heyer, Brunt et al. (2007)

Goldsmith, Heyer, Brunt et al. (2007)

Voids pressurized by magnetic fields...maybe Don Cox is right about the Local Bubble! (whose X-ray emitting gas gets less dense with each passing issue of A&A! (Lallemont et al.)

ON THE DEPOLARIZATION OF DISCRETE RADIO SOURCES BY FARADAY DISPERSION

B. J. Burn

(Received 1965 July 7)

Summary

A study is made of the implications of the recent polarization measurements for the structures of discrete radio sources and the source–observer media. Simple models of wavelength-dependent depolarizing mechanisms are investigated and it is found that most are incompatible with the observations of Gardner & Whiteoak. The models of internal Faraday dispersion predict a lower polarization at 30 cm than is observed. It is suggested that the depolarization of the Crab nebula is produced by Faraday rotation in the filamentary shell that surrounds the nebula. Such filaments could also exist in the outer regions of extragalactic sources.

A complex number representation is used for the state of linear polarization and a Faraday dispersion function is defined to describe the distribution of polarized radiation with respect to Faraday depth. The persistence of polarization at 30 cm, after partial depolarization between 10 cm and 20 cm, implies that the radiation is spread over a large range of Faraday depths. The observed linearity of the plot of the angle of polarization against wavelength squared for most sources implies that it is justifiable to make an assumption which enables one to calculate the Faraday dispersion function of a source from the dependence of its polarization on wavelength.

Estimates are given for upper limits to the densities of internal ionized gases in the sources for which we have polarization measurements.

We write $\epsilon(\mathbf{r}, \lambda)$ for the power radiated at wavelength λ from unit volume at $\mathbf{r}$ per steradian in the direction of the observer. Neglecting the bandwidth, beamwidth and index effects (10), it follows that the observed polarization of the integrated emission from a source is

$$P(\lambda^2) = \frac{\int\int_{\text{source}} \epsilon(\mathbf{r}, \lambda) p(\mathbf{r}) e^{2i\{\alpha(\mathbf{r}) + \phi(\mathbf{r})\lambda^2\}} \, ds \, d\Omega}{\int\int_{\text{source}} \epsilon(\mathbf{r}, \lambda) \, ds \, d\Omega}, \tag{4}$$

where $d\Omega$ is an element of solid angle about $\mathbf{k}$.

It would be very convenient to be able to invert this transform and so obtain the Faraday dispersion function from the relation

$$F(\phi) = \pi^{-1} \int_{-\infty}^{\infty} P(\lambda^2) e^{-2i\phi\lambda^2} \, d(\lambda^2). \tag{12}$$

However, to evaluate this integral we must know $P(\lambda^2)$ for $\lambda^2 < 0$, and this is not an observable quantity. It is readily seen from equation (11) that this is the polarization we would observe if all of the Faraday rotation were in the opposite sense (i.e. if all the magnetic fields were reversed).

Faraday rotation measure synthesis⋆

M. A. Brentjens[1,2] and A. G. de Bruyn[2,1]

[1] Kapteyn Astronomical Institute, University of Groningen, PO Box 800, 9700 AV Groningen, The Netherlands
e-mail: m.a.brentjens@astro.rug.nl
[2] ASTRON, PO Box 2, 7990 AA Dwingeloo, The Netherlands

Received 4 March 2005 / Accepted 20 June 2005

ABSTRACT

We extend the rotation measure work of Burn (1966, MNRAS, 133, 67) to the cases of limited sampling of λ^2 space and non-constant emission spectra. We introduce the rotation measure transfer function (RMTF), which is an excellent predictor of $n\pi$ ambiguity problems with the λ^2 coverage. Rotation measure synthesis can be implemented very efficiently on modern computers. Because the analysis is easily applied to wide fields, one can conduct very fast RM surveys of weak spatially extended sources. Difficult situations, for example multiple sources along the line of sight, are easily detected and transparently handled. Under certain conditions, it is even possible to recover the emission as a function of Faraday depth within a single cloud of ionized gas. Rotation measure synthesis has already been successful in discovering widespread, weak, polarized emission associated with the Perseus cluster (de Bruyn & Brentjens 2005, A&A, 441, 931). In simple, high signal to noise situations it is as good as traditional linear fits to χ versus λ^2 plots. However, when the situation is more complex or very weak polarized emission at high rotation measures is expected, it is the only viable option.

Key words. methods: data analysis – techniques: polarimetric – magnetic fields – polarization – ISM: magnetic fields – Cosmology: large-scale structure of Universe

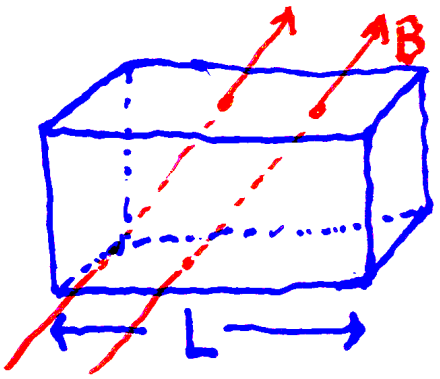

$\phi_{tot} = 0.8\, B_{\parallel} n_e L \lambda^2$

2. FARADAY DEPOLARIZATION

Consider a simple box along the line of sight in which the magnetic field and relativistic electron density (and hence the synchrotron emissivity) are uniform; also, the thermal electron density is uniform, so that the Faraday rotational angle increases linearly with distance into the source. The total Faraday rotation through the whole source is ϕ_{tot} (which varies as λ^2) and the intrinsic degree of linear polarization of the synchrotron radiation is P_s. Typically, $P_s \approx 0.7$. Then the observed linear polarization P_{obs} from the b ox is

$$P_{obs} = P_s \frac{\sin(\phi_{tot})}{\phi_{tot}}$$

and the observed angle of polarization is

$$\phi_{obs} = \tan^{-1}\left(\frac{1}{2}\tan(\phi_{tot})\right)$$

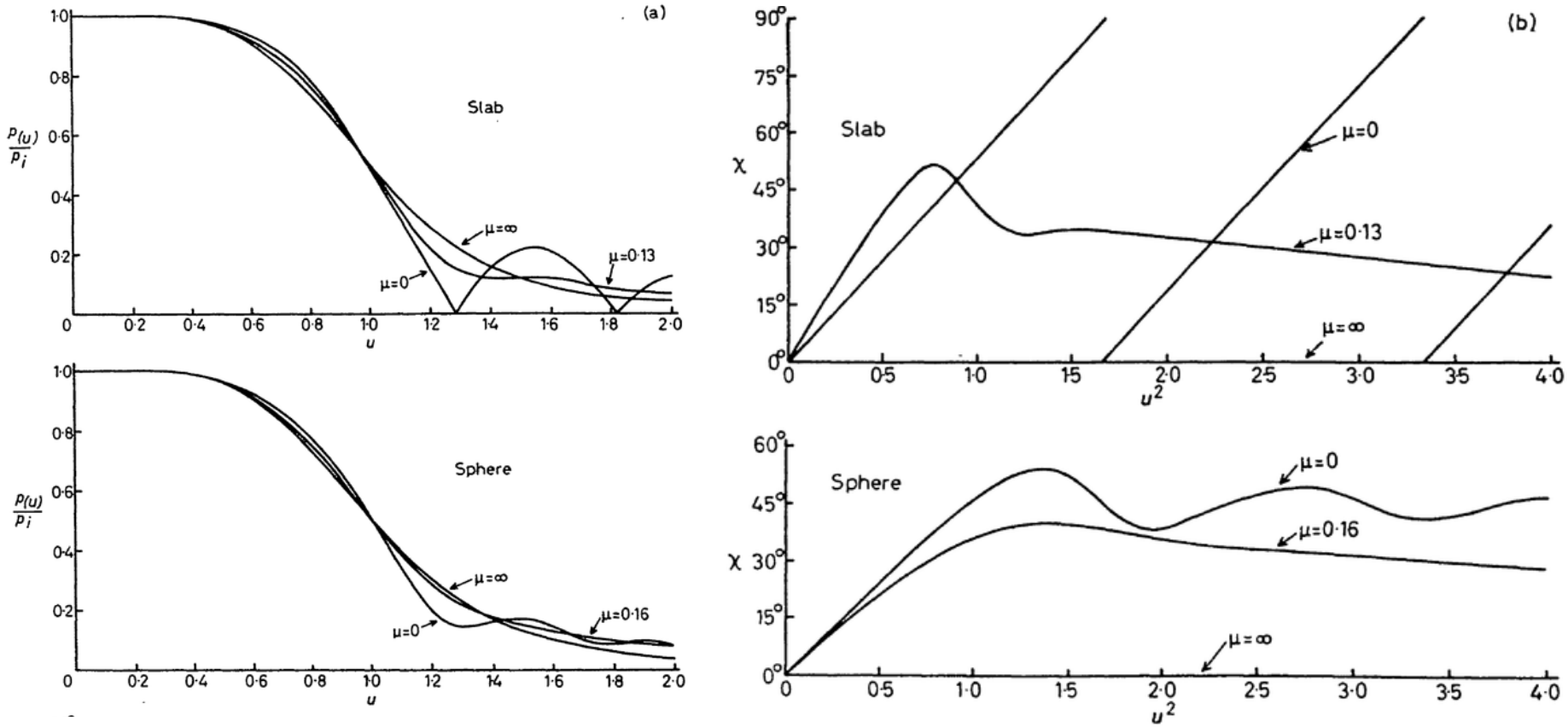

FIG. 2. *Polarization of models of internal Faraday dispersion.* (*a*) *Degree of polarization*; (*b*) *angle of polarization.*

Bpar:

Zeeman splitting

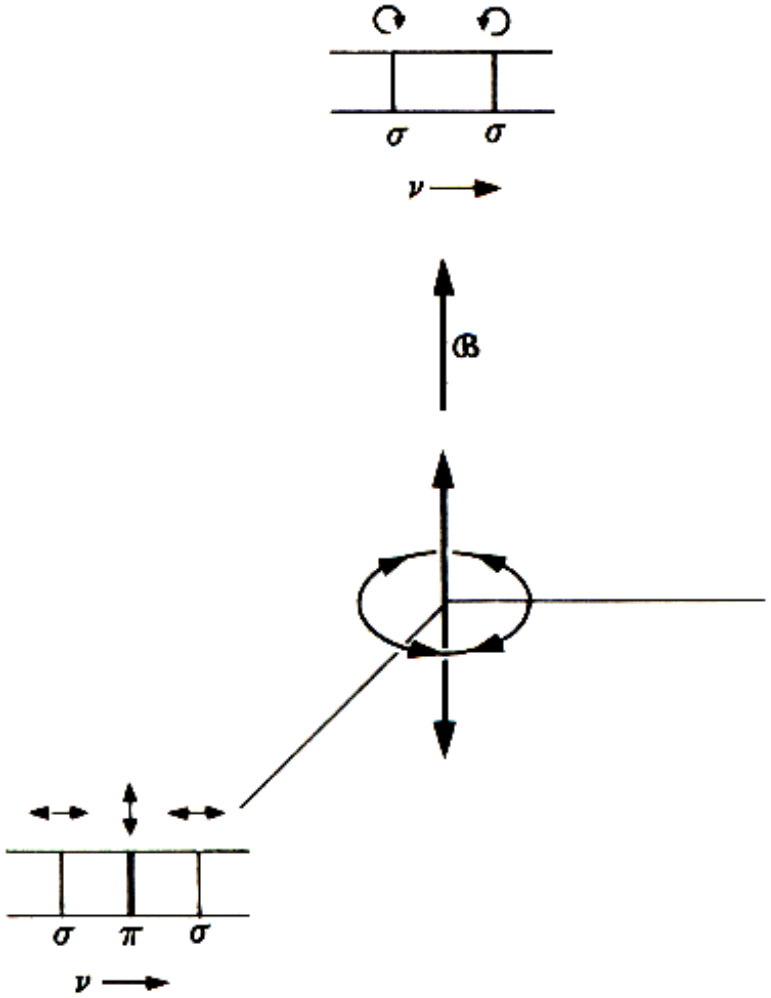

FIG. 10–5. Polarization of light in the spectral lines produced by the Zeeman effect.

3. ZEEMAN SPLITTING

The classical description of the normal Zeeman effect considers the electron in orbit around the atomic nucleus; let's take H, with $Z = 1$. For $B = 0$, the angular frequency of the orbit is $\omega_0 = \left[\frac{e^2}{R^3 m_e}\right]^{1/2}$. For $B \neq 0$, The $F = ma$ equation for the orbit is

$$m_e \omega^2 R = \underbrace{m_e \omega_0^2 R}_{central\ force} \pm \underbrace{\frac{evB}{c}}_{Lorentz\ force}$$

for $\frac{eB}{2mc} \ll \omega_0$ we find

$$\Delta\omega = \omega - \omega_0 = \frac{eB}{2mc}$$

We usually write the splitting in terms of the Bohr magneton μ_e, which is the angular momentum of a classical electron in the first Bohr orbit:

$$\mu_e = \frac{e\bar{h}}{2m_e c}$$

so for species with nonzero angular momentum or spin (e.g., Hydrogen and a few molecules like OH) the frequency offset is

$$\Delta\nu_{zmn} = \frac{g\mu_e}{h} B = 1.4gB \text{ Hz}$$

where g is the Landé g factor (equals unity for Hydrogen). For species without electronic angular momentum or spin, which is most molecules, μ_e gets replaced by the nuclear magneton μ_{nuc}, which is smaller by a factor ~ 1800.

OH maser W75: The only Zeeman triplet known...

FULL-POLARIZATION OBSERVATIONS OF OH MASERS IN MASSIVE STAR-FORMING REGIONS. II. MASER PROPERTIES AND THE INTERPRETATION OF POLARIZATION

VINCENT L. FISH[1]
Harvard-Smithsonian Center for Astrophysics, 60 Garden Street, Cambridge, MA 02138; and National Radio Astronomy Observatory, P. O. Box O, 1003 Lopezville Road, Socorro, NM 87801; vfish@nrao.edu

AND

MARK J. REID
Harvard-Smithsonian Center for Astrophysics, 60 Garden Street, Cambridge, MA 02138; reid@cfa.harvard.edu
Received 2005 December 16; accepted 2006 January 24

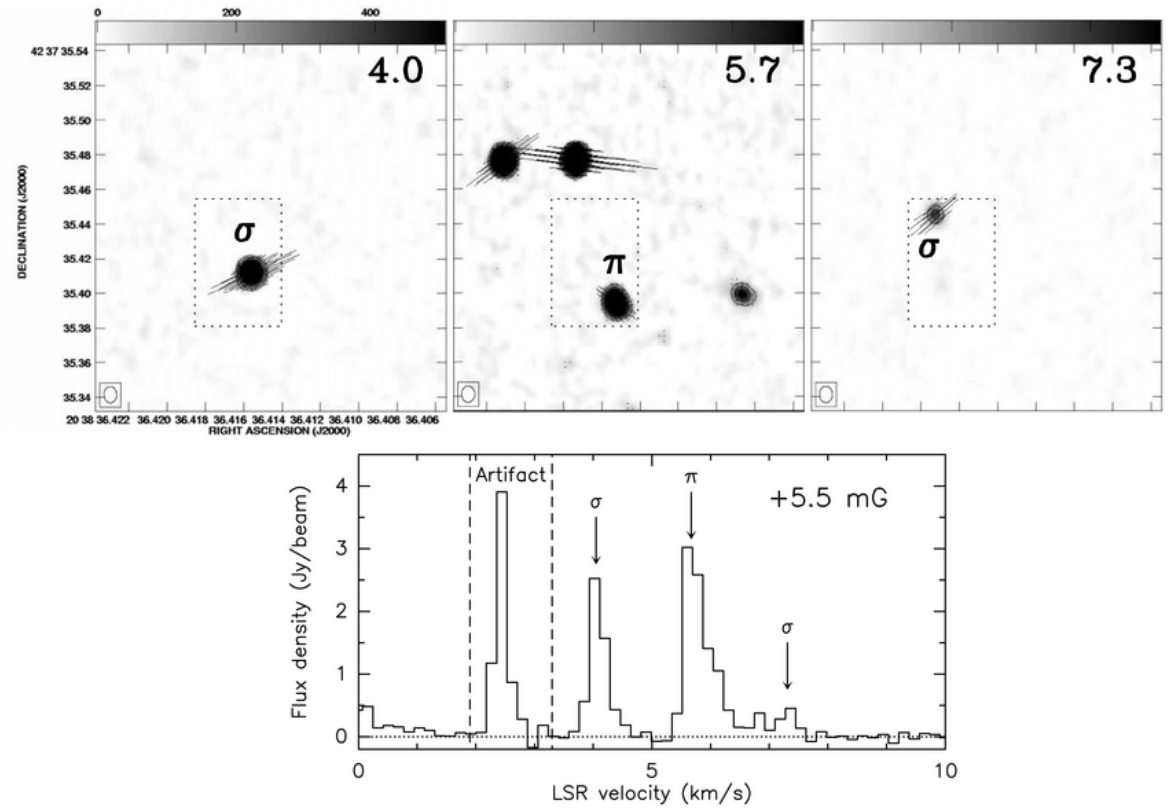

FIG. 1.—Zeeman triplet in W75 N. *Top*: Contour maps of the three Zeeman components with polarization vectors included. Note that the polarization vectors of the σ-components are roughly perpendicular to that of the π-component. LSR velocities in km s^{-1} are shown in the top right of each panel. *Bottom*: Spectrum of the dotted box region in the upper plots. The feature labeled "artifact" is due to the sidelobe of a very strong maser spot outside the region shown. The velocities of the three marked components are consistent with a +5.5 mG magnetic field.

The pi components are almost never seen. The two sigma components are seen as a doublet when splitting/linewidth is large, which happens ONLY in OH masers. Splitting then gives the total B.

Usual case: splitting/linewidth << 1

Zeeman Splitting

Splitting << linewidth even at 100 mG.

Zeeman effect detected as a frequency offset Δv_Z between LH and RH circular polarizations in the spectral line.

We fit Stokes V to derivative of Gaussians to determine B_{los}

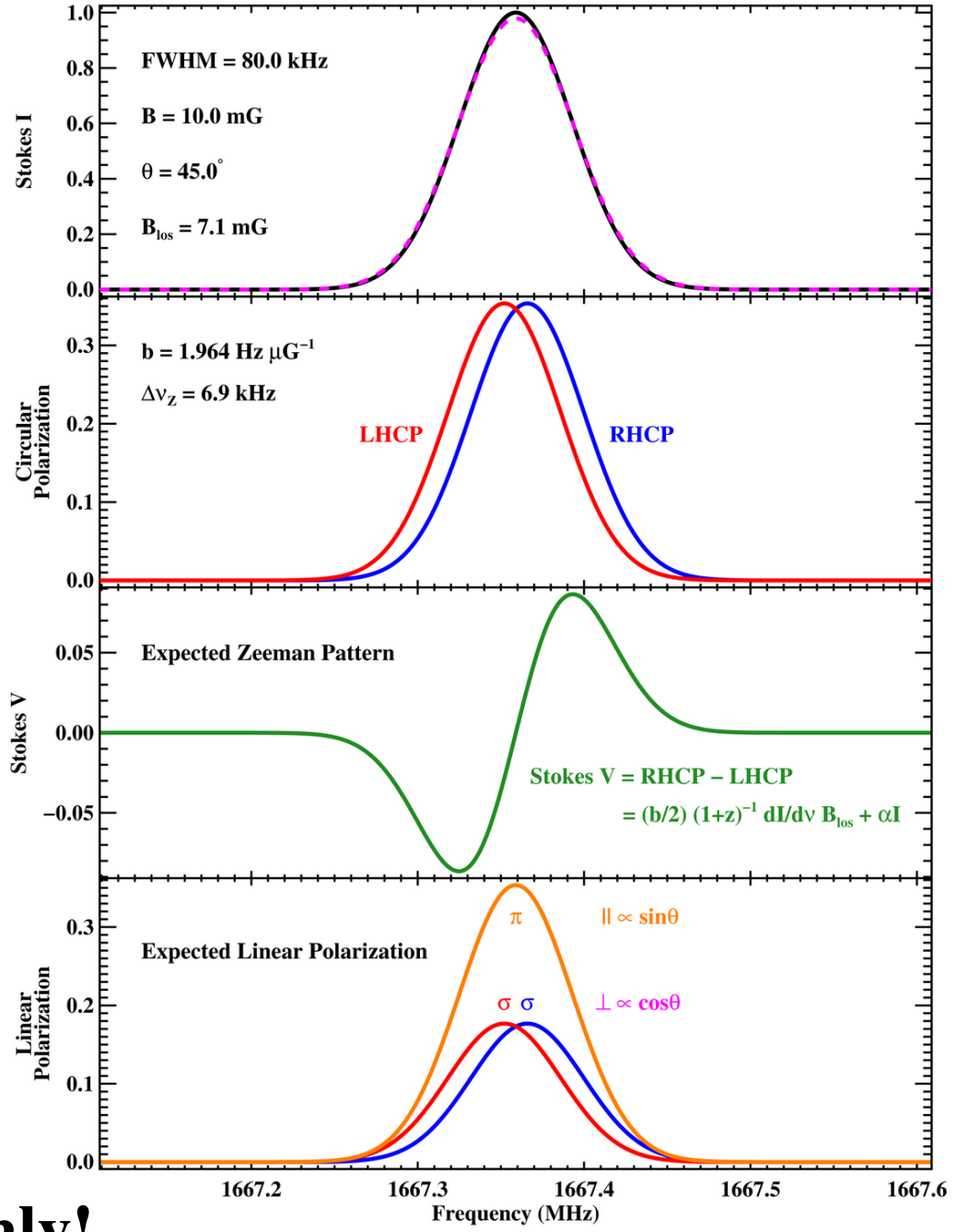

Note: los component only!

splitting << linewidth SUMMARY:

*** Circular Polarization (Stokes V) goes as [splitting/linewidth] and gives line-of-sight component only**

*** Linear Polarization (Stokes Q, U) goes as [splitting/linewidth]^2**

*** for [splitting/linewidth] << 1, circular is already too weak to see easily. Forget about linear in this case!**

Two high S/N examples of Zeeman splitting for HI absorption:

Cas A (dense cloud near star formation): B_{los} = 10, 25 μG

Tau A (CNM NOT near star formation): B_{los} = 7, -3 μG

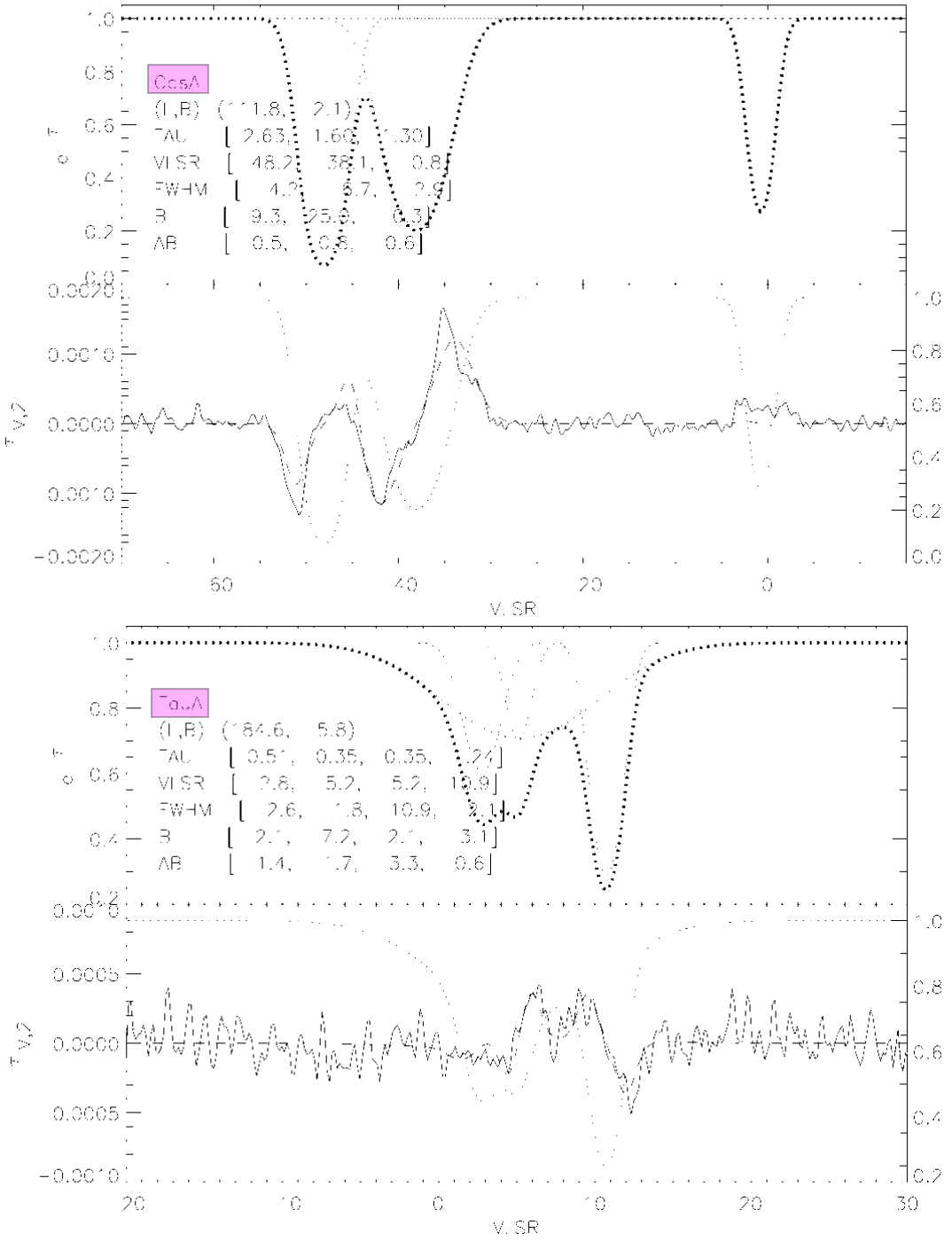

Heiles et al., in "Protostars and Planets III"

MAGNETIC FIELDS IN STAR-FORMING REGIONS: OBSERVATIONS

CARL HEILES, ALYSSA A. GOODMAN, CHRISTOPHER F. McKEE
University of California, Berkeley

and

ELLEN G. ZWEIBEL
University of Colorado, Boulder

We review the observational aspects of magnetic fields in dense, star-forming regions. First we discuss ways to observe the field. These include direct methods, which consist of the measurement of both linear and circular polarization of spectral line and continuum radiation; and indirect methods, consisting of the angular distribution of H_2O masers on the sky and the measurement of ambipolar diffusion. Next we discuss selected observational results, focusing on detailed discussions of a small number of points rather than a general discussion that covers the entire front. First we discuss the Orion/BN-KL region in detail, both on the small and large scales. Next we discuss the derivation of the complete magnetic vector, including both the systematic and fluctuating components, for a large sample of Zeeman and linear polarization measurements for the L204 dark cloud. Third we discuss the virial theorem as it applies to dark clouds in general and one dark cloud, Barnard 1, in particular. Finally we critically discuss the numerous claims for alignment of elongated structural features with the plane-of-the-sky component of the magnetic field, and find that many of these have not been definitively established.

This review contains a comprehensive table of Zeeman-useful molecules

TABLE I

Candidates for Zeeman Observations

		ν [GHz] (a)	(b)	b [Hz μG^{-1}] (c)	n [cm^{-3}] (d)	Δv [km s^{-1}] (e)	B [μG] (f)	$\lvert V_{max}\rvert/T_A$ (g)
Atomic Transitions:								
HI	$^2S_{\frac{1}{2}}$, F=1–0	1.420	1, 1	2.80	1×10^2	2.0	10	2×10^{-3}
HI	recombination lines[h]	1–400	16, 17	2.80	10^2–10^7	2.0	100?	$\lesssim 5 \times 10^{-3}$
Molecular Transitions, Splitting Determined by Electronic Magnetic Moment:								
CH	$^2\Pi_{3/2}$, J=3/2, F=2–2	0.7017	2, 12	1.96	1×10^6	2.0	1020	3×10^{-1}
CH	$^2\Pi_{3/2}$, J=3/2, F=1–1	0.7248	2, 12	3.27	1×10^6	2.0	1020	5×10^{-1}
OH	$^2\Pi_{3/2}$, J=3/2, F=1–2	1.612	3, 3	1.31	5×10^3	1.0	36	6×10^{-3}
OH	$^2\Pi_{3/2}$, J=3/2, F=1–1	1.665	3, 3	3.27	5×10^3	1.0	36	2×10^{-2}
OH	$^2\Pi_{3/2}$, J=3/2, F=2–2	1.667	3, 2	1.96	5×10^3	1.0	36	9×10^{-3}
OH	$^2\Pi_{3/2}$, J=5/2, F=2–1	1.720	3, 3	1.31	5×10^3	1.0	36	6×10^{-3}
OH	$^2\Pi_{3/2}$, J=5/2, F=2–3	6.016	3, 3	0.68	5×10^3	1.0	36	9×10^{-4} (p)
OH	$^2\Pi_{3/2}$, J=5/2, F=2–2	6.031	3, 3	1.58	5×10^3	1.0	36	2×10^{-3} (p)
OH	$^2\Pi_{3/2}$, J=5/2, F=3–3	6.035	3, 3	1.13	5×10^3	1.0	36	1×10^{-3} (p)
OH	$^2\Pi_{3/2}$, J=5/2, F=3–2	6.049	3, 3	0.68	5×10^3	1.0	36	9×10^{-4} (p)
C_4H	N=1–0, J=3/2–1/2, F=2–1	9.4976	4, 13	1.40	3×10^4	0.5	44	3×10^{-3}
C_4H	N=2–1, J=5/2–3/2, F=2–1	19.0147	4, 13	1.30	3×10^4	0.5	44	1×10^{-3}
C_4H	N=2–1, J=5/2–3/2, F=3–2	19.0151	4, 13	0.93	3×10^4	0.5	44	9×10^{-4}
C_2S	$J_N = 1_0$–0_1	11.12	5, 14	0.84[l]	1×10^5	0.5	81	3×10^{-3}
SO	$J_N = 2_2 - 1_1$	86.094	6, 6	0.47[m]	5×10^4	1.0	114	1×10^{-4}
O_2	N=1, J=1–0 (above atmosphere)	56.264	7, 8	2.80	5×10^4	0.5	57	1×10^{-3} (q)
O_2	N=1, J=2–1 (above atmosphere)	118.75	7, 8	2.80	5×10^4	0.5	57	6×10^{-4} (q)
CN	N=1–0, J=3/2–1/2, F=3/2–1/2	113.49	8, 8	2.20	1×10^4	1.0	51	2×10^{-4}
CN	N=2–1, J=3/2, F=3/2–5/2	226.33	8, 8	2.60	1×10^4	1.0	51	1×10^{-4}
C_2H	N=1–0, J=3/2–1/2, F=2–1	87.317	9, 13	1.40	1×10^5	2.0	323	6×10^{-4}
Molecular Transitions, Splitting Determined by Nuclear Magnetic Moment:								
OH	$^2\pi_{1/2}$, J=1/2, F=0–1	4.66	3, 3	~ 0.001	1×10^7	2.0	3×10^3	7×10^{-5}
OH	$^2\pi_{1/2}$, J=1/2, F=1–1	4.751	3, 3	~ 0.001	1×10^7	2.0	3×10^3	7×10^{-5}
OH	$^2\pi_{1/2}$, J=1/2, F=1–0	4.766	3, 3	~ 0.001	1×10^7	2.0	3×10^3	7×10^{-5}
H_2O	Hyperfines of $(6_{16} - 5_{23})$	22.235	10, 10	0.0029	1×10^9	2.0	3×10^4	5×10^{-4}
NH_3	Inversion transitions, e.g. JK=33[n]	~78	11, 15	0.00072	1×10^7	2.0	3×10^3	3×10^{-6}

11.119446 CH (Lovas et al. ApJ 399, 326)

ZEEMAN CANDIDATES: $\nu > 60$ GHz

SPECIES	ν_{GHz}	n_{typ}	$B_{\mu G}$ *	$\Delta V_{km/s}$ *	$\lvert V/I \rvert_{max}$
HI RECOMB.	90		10^3	10	$3 \cdot 10^{-3}$
SO	86	$5 \cdot 10^4$	114	1.0	$2.8 \cdot 10^{-4}$
C_2H	87	$1 \cdot 10^5$	323	2.0	$1.1 \cdot 10^{-3}$
CN	113	$1 \cdot 10^4$	51	1.0	$4.1 \cdot 10^{-4}$
O_2	118	$5 \cdot 10^4$	57	0.5	$1.1 \cdot 10^{-3}$

* { ΔV IS "TYPICAL OBSERVED VALUE"
  { B ASSUMED SUCH THAT $\Delta V = \Delta V_{ALF}$.

Zeeman splitting:

Radiative transfer effects

THE ASTROPHYSICAL JOURNAL, 558:L55–L58, 2001 September 1

THE RELATIONSHIP BETWEEN THE CIRCULAR POLARIZATION AND THE MAGNETIC FIELD FOR ASTROPHYSICAL MASERS WITH WEAK ZEEMAN SPLITTING

W. D. WATSON AND H. W. WYLD
Department of Physics, University of Illinois at Urbana-Champaign, 1110 West Green Street, Urbana, IL 61801-3080
Received 2001 June 27; accepted 2001 July 27; published 2001 August 3

ABSTRACT

The relationship between the magnetic field and the circular polarization of astrophysical maser radiation due to the Zeeman effect under idealized conditions is investigated when the Zeeman splitting is much smaller than the spectral line breadth and when radiative saturation is significant. The description of the circular polarization as well as inferences about the magnetic field from the observations are clearest when the rate for stimulated emission is much less than the Zeeman splitting. The calculations here are performed in this regime, which is relevant for some (if not most) observations of astrophysical masers. We demonstrate that the Stokes V parameter is proportional to the Zeeman splitting and that the fractional linear polarization is independent of the Zeeman splitting when the ratio of the Zeeman splitting to the spectral line breadth is small—less than about 0.1. In contrast to its behavior for ordinary spectral lines, the circular polarization for masers that are at least partially saturated does not decrease with increasing angle between the magnetic field and the line of sight until they are nearly perpendicular.

Subject headings: magnetic fields — masers — polarization

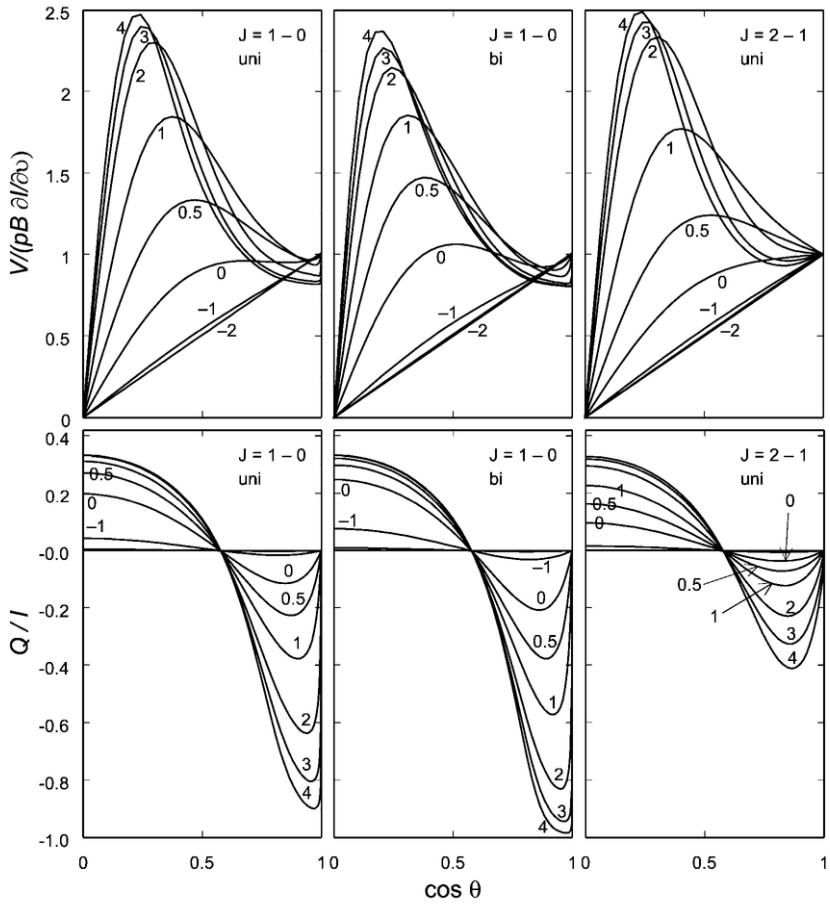

In summary, when the observed masers are believed to be at least somewhat saturated, but when there is no good information about the angle θ or about the exact degree of saturation, simply removing the $\cos\theta$ in equation (1) would seem to provide the best way at present to infer magnetic field strengths from the observed the Stokes V parameter in the weak splitting regime when "non-Zeeman effects" can be ignored. Saturation with $I \gtrsim 10^2$ (and probably even $I \gtrsim 10$) seems unlikely for astrophysical masers. In contrast to the linear polarization, the circular polarization is relatively insensitive to the angular momentum of the molecular states. We emphasize that our results are applicable in detail only to the idealized masing conditions on which the calculations are based (see § 1). In addition to non-Zeeman effects, velocity gradients, anisotropic pumping, and multiple hyperfine components may be present but are not considered here. For example, the 22 GHz masing transition of water probably consists of multiple hyperfine components, and so equation (1) is unlikely to be directly applicable (but see Nedoluha & Watson 1992).

LINEAR AND CIRCULAR POLARIZATION FOR MASERS WITH WEAK ZEEMAN SPLITTINGS

Gerald E. Nedoluha
NRC Cooperative Research Associate
Naval Research Lab
Washington DC 20375-5000

William D. Watson
Loomis Lab of Physics
University of Illinois
Urbana IL 61801

!!!

ABSTRACT

Theory is reviewed for the linear and circular polarization of radiation from astrophysical masers in which the Zeeman splitting $g\Omega$ is much less than the spectral linewidth $\Delta\omega$. When $g\Omega \gtrsim \Gamma$ (the decay rate for the molecular states), polarization – mainly linear – can be generated. New results are presented that describe the generation of circular polarization by intensity dependent (or "false") Zeeman effects. As a result, the magnetic field strengths inferred from the circular polarization of circumstellar SiO masers may be smaller than previous estimates by a factor of 100 or more.

RevMexAA (Serie de Conferencias), **36**, 113–120 (2009)

MAGNETIC FIELDS AND THE POLARIZATION OF ASTROPHYSICAL MASER RADIATION: A REVIEW

W. D. Watson[1]

RESUMEN

Se describen aspectos básicos de la relación entre el campo magnético y la radiación maser polarizada con énfasis en la interpretación del espectro observado. Se da especial atención a tres aspectos – las limitaciones en la aplicabilidad de las soluciones clásicas de Goldreich, Keeley & Kwan (1973), la inferencia de la magnitud del campo magnético a partir de la polarización circular cuando el desdoblamiento Zeeman es mucho menor que el ancho espectral de la línea (especialmente para máseres de SiO), y el significado de la ausencia de componentes del triplete de Zeeman en el espectro de máseres de OH en regiones de formación estelar.

ABSTRACT

Basic aspects of the relationship between the magnetic field and polarized maser radiation are described with the emphasis on interpreting the observed spectra. Special attention is given to three issues – the limitations on the applicability of the classic solutions of Goldreich, Keeley, & Kwan (1973), inferring the strength of the magnetic field from the circular polarization when the Zeeman splitting is much less than the spectral linebreadth (especially for SiO masers), and the significance of the absence of components of the Zeeman triplet in the spectra of OH masers in regions of star formation.

Key Words: circumstellar matter — ISM: clouds — magnetic fields — masers — polarization

More radiative transfer:

The Goldreich-Kylafis effect

LINEAR POLARIZATION -- FUNDAMENTALS.

CLASSICAL VIEWPOINT: A CLASSICAL ATOM IN A MAGNETIC FIELD:

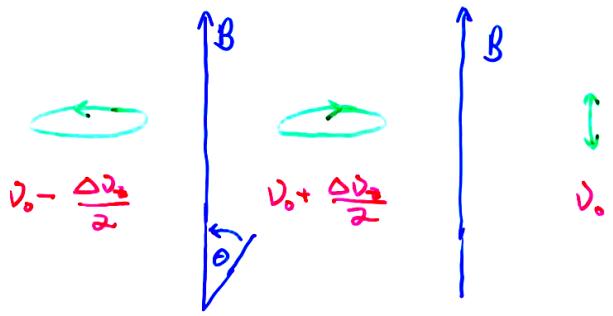

σ COMPONENTS

π COMPONENT

CLASSICAL E.M. RADIATION PATTERN → $I_\sigma \propto 1+\cos^2\theta$

$I_\pi \propto \sin^2\theta$

→ THE EINSTEIN "A" AND "B" COEFFICIENTS DEPEND UPON θ.

CONSIDER A CLOUD ILLUMINATED BY AN ANISOTROPIC RADIATION FIELD:

↑ ANISOTROPIC RADIATION AT THE TRANSITION FREQUENCY

WITH $\theta = 0$, THE π COMPONENT IS NOT AFFECTED BY THE RADIATION. PHOTON TRAPPING IS LESS EFFECTIVE FOR π COMPONENTS. RESULT:

- σ COMPONENTS ARE STRONGER IN EMISSION THAN THE π COMPONENT.
- THERE IS NO NET CIRCULAR POLARIZATION, BECAUSE THE 2 σ COMPONENTS HAVE EQUAL INTENSITIES.
- BUT, BECAUSE σ COMPONENTS ARE STRONGER THAN π COMPONENTS, EMISSION IS LINEARLY POLARIZED ⊥ TO B.
- WITH $\theta = 90°$, POLARIZATION IS ∥ TO B.
- IN GENERAL, POLARIZATION IS EITHER ∥ OR ⊥ TO B.
- SOLVING A REALISTIC CASE REQUIRES COMPLICATED RADIATIVE TRANSFER; NUMERICAL MODELS OR EXTREMELY ALGEBRAICLY CUMBERSOME SOLUTIONS.

POLARIZATION OF INTERSTELLAR RADIO-FREQUENCY LINES AND MAGNETIC FIELD DIRECTION

NIKOLAOS D. KYLAFIS
Institute for Advanced Study, Princeton
Received 1982 June 1; accepted 1982 September 22

ABSTRACT

Analytic expressions are presented for the amount of polarization and the brightness temperature expected in radio and infrared lines from sources undergoing one-dimensional or two-dimensional axisymmetric collapse *or* expansion. The results are applied to (*a*) a molecular cloud collapsing primarily along one direction and (*b*) an expanding circumstellar envelope. It is found that the amount of polarization has a maximum of about 18% for a one-dimensional velocity field and about half of that for a two-dimensional field. Specific examples are given that pertain to CO. The various parameter regimes are explored and suggestions are made regarding the selection of molecules and sources to be observed. A relation is given between the polarization vector and the magnetic field direction.

Subject headings: interstellar: molecules — molecular processes — polarization — radiative transfer — radio sources: lines

TWO EXAMPLES BY KYLAFIS: BOTH AXISYMMETRIC+LVG.

1-D

V ∥ TO AXIS

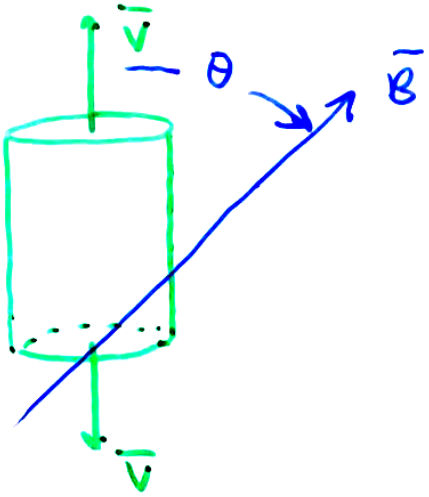

2-D

V⊥ TO AXIS

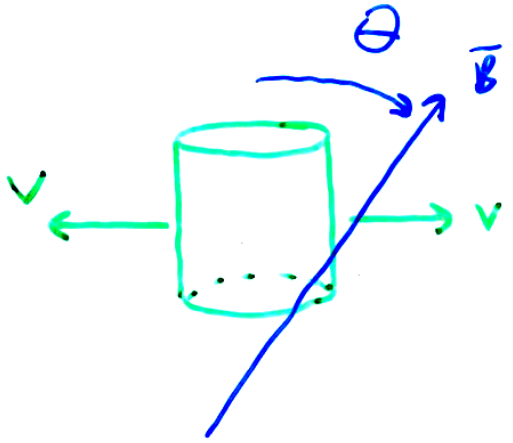

ASSUMED A CO CLOUD WITH $T_k = 30$ K.

Plots of %pol vs line optical depth for the two cases . High polarizations are possible!

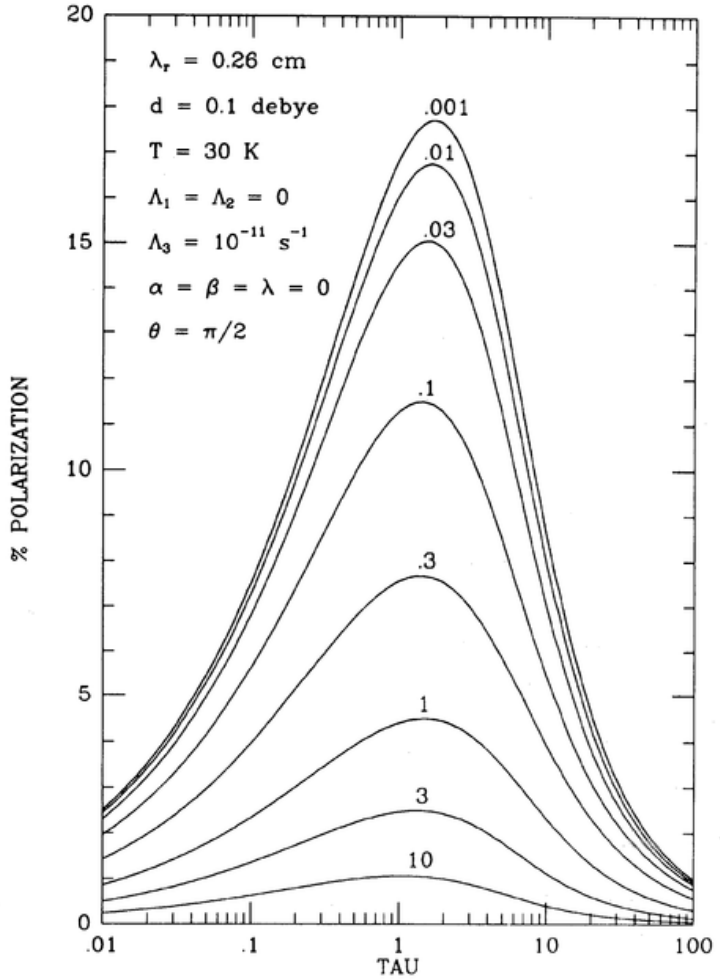

FIG. 1*a*

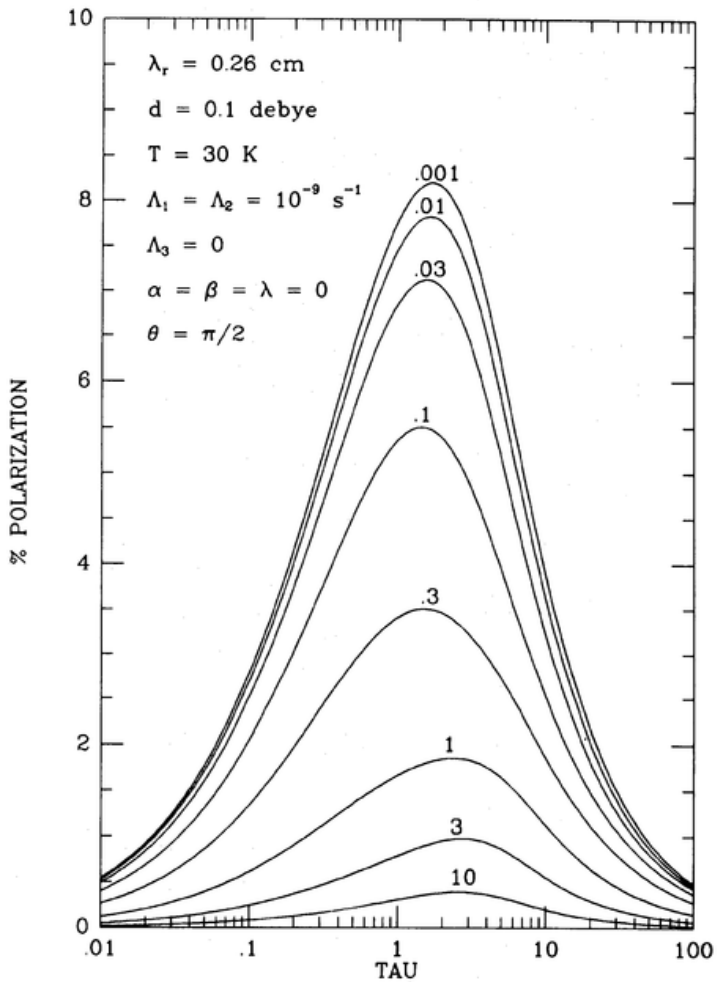

FIG. 1*b*

FIG. 1.—(*a*) Percent polarization as a function of mean optical depth expected for CO $J = 1$ to $J = 0$ transitions in a one-dimensional velocity field. The numbers on the curves give the corresponding values of $C/A_{a,b} = C'/A_{a,b}$. (*b*) Same as Fig. 1*a* but for a two-dimensional velocity field.

But the pol position angle is ambiguous: either par or perp to Bperp

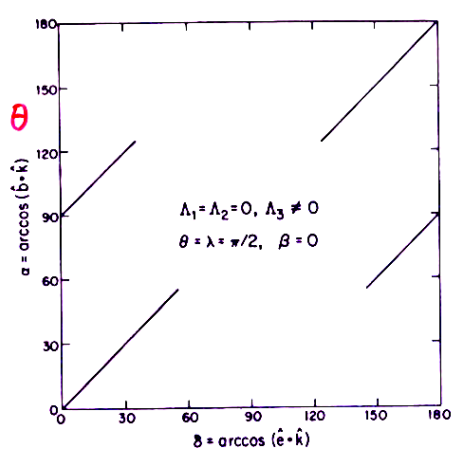

FIG. 5a

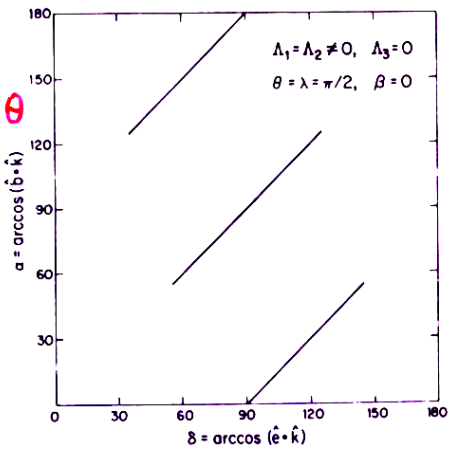

FIG. 5b

FIG. 5.—(*a*) Relationship between observed polarization vector and magnetic field direction in a one-dimensional velocity field. (*b*) Same as Fig. 5*a* but for a two-dimensional velocity field.

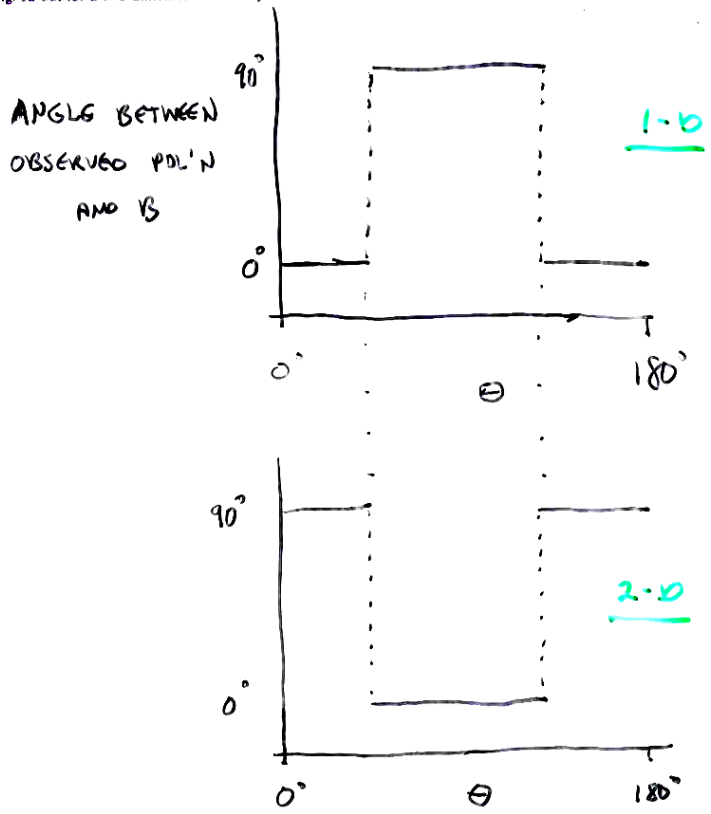

...E POLARIZATION OF MOLECULAR LINES AT RADIO FREQUENCIES: THE CASE OF DR 21(OH)

P. C. Cortes,[1] R. M. Crutcher,[1] and W. D. Watson[2]

Received 2005 February 23; accepted 2005 April 7

ABSTRACT

We present polarization observations in DR 21(OH) from thermal dust emission at 3 mm and from CO $J = 1 \rightarrow 0$ line emission. The observations were obtained using the Berkeley-Illinois-Maryland Association (BIMA) array. Lai et al. observed this region at 1.3 mm for the polarized continuum emission and also measured the CO $J = 2 \rightarrow 1$ polarization. Our continuum polarization results are consistent with those of Lai et al. However, the direction of the linear polarization for the $J = 1 \rightarrow 0$ is perpendicular to that of the CO $J = 2 \rightarrow 1$ polarization. This unexpected

INTERFEROMETRIC MAPPING OF MAGNETIC FIELDS IN STAR-FORMING REGIONS. III. DUST AND CO POLARIZATION IN DR 21(OH)

Shih-Ping Lai,[1] José M. Girart,[2] and Richard M. Crutcher
Astronomy Department, University of Illinois, 1002 West Green Street, Urbana, IL 61801;
slai@astro.umd.edu, jgirart@am.ub.es, crutcher@astro.uiuc.edu

Received 2002 December 2; accepted 2003 July 29

ABSTRACT

We present the polarization detections in DR 21(OH) from both the thermal dust emission at 1.3 mm and the CO $J = 2 \rightarrow 1$ line obtained with the Berkeley-Illinois-Maryland Association array. Our results are consistent with the prediction of the Goldreich-Kylafis effect that the CO polarization is either parallel or perpendicular to the magnetic field direction. The detection of the polarized CO emission is over a more extended

Note that the dust pol PA (perp to the TRUE Bperp) is either aligned or orthogonal to the CO pol PA

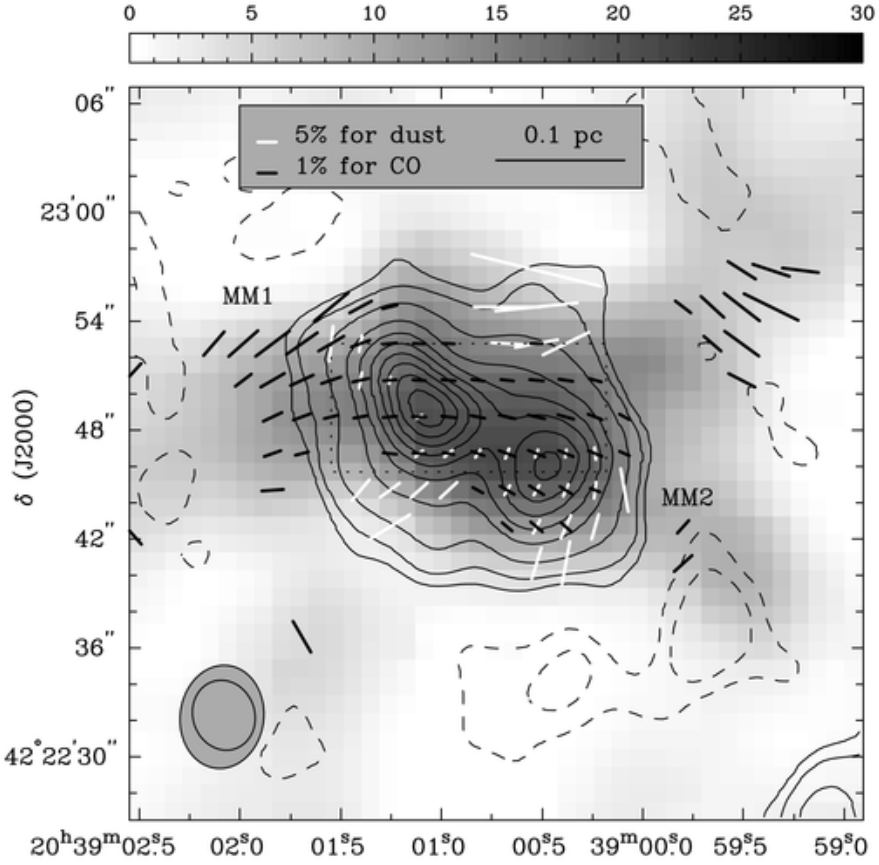

CO (2 → 1) [black]
Dust (1.3mm) [white]
Grayscale is dust (1.3mm)

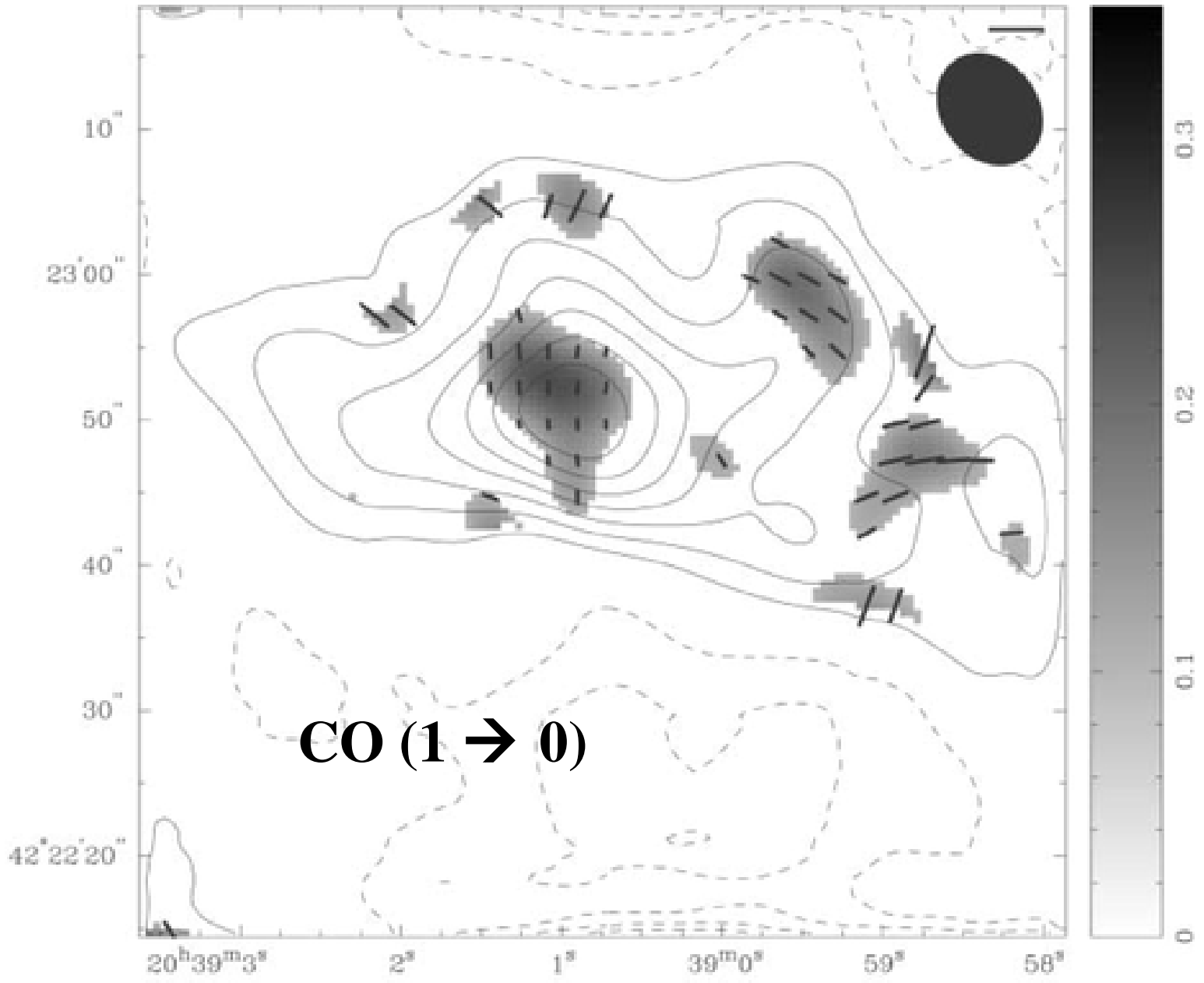
10"
23'00"
50"
40"
30"
42°22'20"
20h39m3s
2s
1s
39m0s
59s
58s
0.3
0.2
0.1
0
CO (1 → 0)

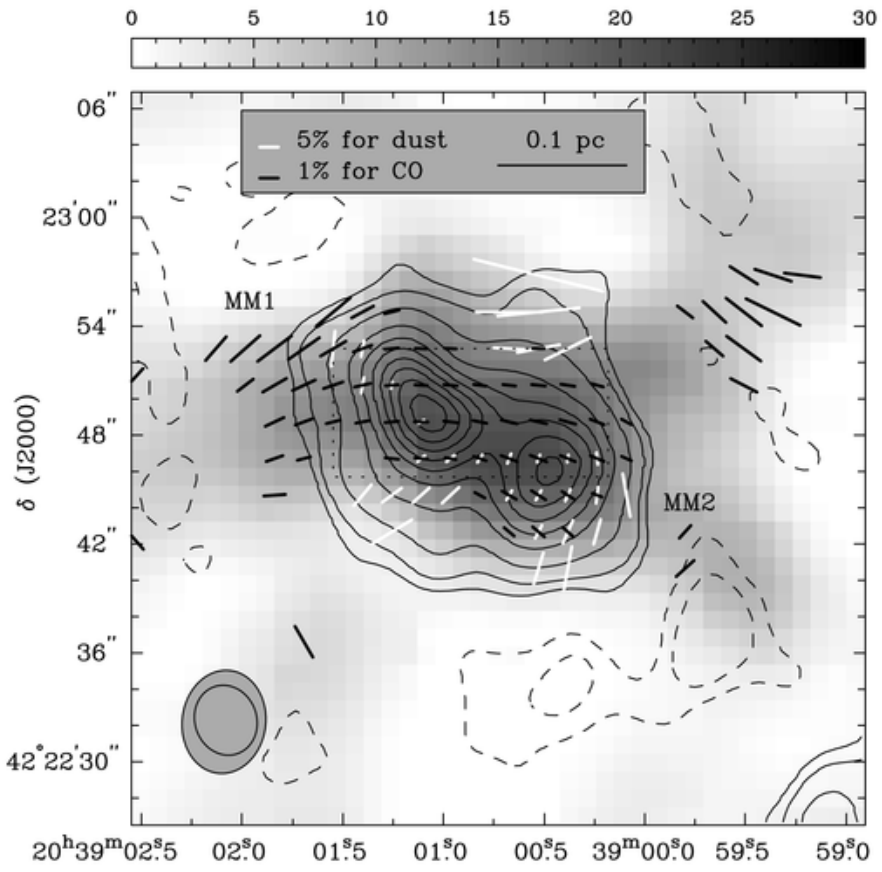

CO (2 → 1) [black]
Dust (1.3mm) [white]
Grayscale is dust (1.3mm)

HOW ABOUT LINEAR BIREFRINGENCE ???? (CONVERTS LINEAR TO CIRCULAR)

H_2O

THIS QUESTION IS RELEVANT MAINLY FOR MASERS AND, POSSIBLY, ABSORPTION LINES.

FUNDAMENTALS:

WE'VE SEEN ALREADY THAT, BECAUSE OF DIFFERING OPACITIES PRODUCED BY AN ANISOTROPIC RADIATION FIELD, THAT THE ABSORPTION COEFFICIENT $K_{\parallel} \neq K_{\perp}$, FROM KRAMERS-KRONIG RELATIONSHIP, THIS MEANS THAT

$$v_{\phi,\parallel} \neq v_{\phi,\perp} \qquad \text{(PHASE VELOCITY FOR E-M)}$$

CONSIDER AN INCIDENT LINEARLY POLARIZED WAVE AT 45° TO $\overline{B}$:

AS THE WAVE PROPAGATES, THE PHASE DIFFERENCE BETWEEN $E_{\parallel}$ AND $E_{\perp}$ VARIES FROM 0° TO 360° .... THUS PRODUCES CIRCULAR POLARIZATION, IF THE PHASE ANGLE $\neq 0°$ OR $n \cdot 180°$.

NOTE: IF THE POLARIZATION OF THE INCIDENT RADIATION IS PRODUCED BY THE RADIATIVE TRANSFER EFFECTS OF ABOVE, THEN CIRCULAR POL'N IS NOT PRODUCED BECAUSE THE INCIDENT POL'N IS EITHER $\parallel$ OR $\perp$ TO B.

HOWEVER, IF THE FIELD "TWISTS" ALONG THE LINE OF SIGHT, SOME CONVERSION TO CIRCULAR CAN OCCUR. THIS OCCURS IN THE SAME REGION IN WHICH LINEAR POL'N IS BEING PRODUCED. THE CIRCULAR POL'N IS A 2^{nd} ORDER EFFECT. THUS, IN THE ABSENCE OF AN EXTERNAL SOURCE OF LINEAR POL'N, WE EXPECT

$$\frac{V_{MAX}}{I} \lesssim \left[\frac{(Q^2+U^2)^{1/2}}{I} \right]^2 \qquad (<<1)$$

EXAMPLE:

WATER MASERS!

$$\frac{V_{MAX}}{I} \cong 10^{-3}$$

IT MIGHT BE ZEEMAN SPLITTING: $B \cong 35$ mG.

IT MIGHT BE LINEAR BIREFRINGENCE!

Bperp:
Aligned grains
and the
Chandrasekhar /Fermi mechanism

POLARIZED THERMAL EMISSION FROM GRAINS -

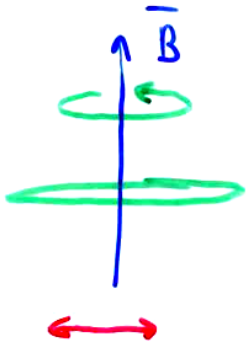

NEEDLE-LIKE GRAIN

- GRAIN SIZE $<< \lambda$, SO POLARIZATION $\parallel$ TO NEEDLE $\perp$ TO $\overline{B}$.

- THE ALIGNMENT OF GRAINS WITH $\overline{B}$ IS ESSENTIALLY PERFECT. THUS, THE POLARIZED INTENSITY PROVIDES NO INFO ON B.

- GRAIN PROPERTIES SUCH THAT THE PDL'N SHOULD BE λ-INDEPENDENT FOR $\lambda \lesssim$ IR. UNLESS GRAIN TEMPERATURES VARY SIGNIFICANTLY ALONG THE LINE OF SIGHT, IR AND mm WAVE RESULTS SHOULD BE SIMILAR.

4. GRAIN ALIGNMENT WITH THE MAGNETIC FIELD

Grains, especially large ones, are very well-aligned with the magnetic field as revealed by polarization of absorbed starlight and polarization of IR emission. These linear polarizations reveal the orientation of the *plane-in-the-sky* projected field, denoted $B_\perp$.

Grain Alignment with the Magnetic Field is an exceedingly complicated problem in solid state physics. Draine's new ISM textbook contains a good summary. Some of the major solid-state physics players include

- Alignment of the Grain body with the angular momentum. The grain rotates around its largest moment of inertia to minimize the rotational energy $\frac{J^2}{I}$ for constant J. The major dissipation processes are associated with the Barnett effect.
- Alignment of the angular momentum and magnetic field. A major player is suprathermal grain rotation, which is produced by systematic torques centered on the grain. Torques are produced by radiation (the angular momentum of photons in an anisotropic radiation field), H_2 formation sites, enhanced accreting-atom sites, photoelectric emission sites. "Crossover events" and "thermal flipping" prevent good alignment of small grains.

The Bottom Line: Needle-like grains rotate around a short axis so that the projected needle is longest perpendicular to the field. This, in turn, results in

- Polarization of absorbed starlight lies *parallel* to $B_\perp$.
- Polarization of emitted IR lies *perpendicular* to $B_\perp$.

MAGNETIC FIELDS IN SPIRAL ARMS

S. CHANDRASEKHAR AND E. FERMI
University of Chicago
Received March 23, 1953

ABSTRACT

In this paper two independent methods are described for estimating the magnetic field in the spiral arm in which we are located. The first method is based on an interpretation of the dispersion (of the order of 10°) in the observed planes of polarization of the light of the distant stars; it leads to an estimate of $H = 7.2 \times 10^{-6}$ gauss. The second method is based on the requirement of equilibrium of the spiral arm with respect to lateral expansion and contraction: it leads to an estimate of $H = 6 \times 10^{-6}$ gauss.

As we observe distant stars in a direction approximately perpendicular to the spiral arm, it appears that the direction of polarization is only approximately parallel to the arm. There are indeed quite appreciable and apparently irregular fluctuations in the direction of polarization of the distant stars.[4] This would indicate that the magnetic lines of force are not strictly straight and that they may be better described as "wavy" lines. The mean angular deviation of the plane of polarization from the direction of the spiral arm appears to be about $a = 0.2$ radians.[4] There must clearly be a relation between this angle, a, and the strength of the magnetic field, H. For, if the magnetic field were sufficiently strong, the lines of force would be quite straight and a would be very small; on the other hand, if the magnetic field were sufficiently weak, the lines of force would be dragged around in various directions by the turbulent motions of the gas masses in the spiral arm and a would be large. To obtain the general relation between a and H, we proceed as follows:

Zweibel (1996) gives a clear, complete, and no-small-angle approximation treatment

3. Field Strengths from Polarization Measurements

There appears to be no correlation between measured polarization and field strength, within the range of field strengths commonly encountered in the ISM. However, Chandrasekhar & Fermi (1953) realized that measurements of the dispersion in angle of polarization could be combined with observations of the dynamics in order to estimate the magnetic field strength. Their method was shortly afterward applied to star clusters (Hall & Serkowski 1963) and has been applied more recently by Gonatas et al. (1990) to the Orion molecular cloud and by Hildebrand et al. (1990), Morris et al. 1992, and Hildebrand et al. (1993) to conditions near the Galactic Center.

The method rests on several assumptions. In essence, it is an application of the equipartition principle for small amplitude fluctuations in a medium dominated by magnetic forces. Consider a mean magnetic field of magnitude B_o embedded in a medium of constant density ρ. Small amplitude, transverse fluctuations ΔB_t are accompanied by motions of amplitude $\Delta V_{\|}$, which are parallel to ΔB_t. It can be shown from the linearized equation of motion and magnetic induction equation that the mean values of ΔB_t and ΔV_t are related to each other by

$$\langle \Delta V_t^2 \rangle = \frac{\langle \Delta B_t^2 \rangle}{4\pi\rho}, \tag{7}$$

i.e., there is equipartition between the averaged kinetic and magnetic fluctuation energy densities. The magnetic energy should here be regarded as potential energy, other forms of which can be added to the right-hand side of eq. (7).

Equation (7) is equivalent to

$$\frac{\langle \Delta V_t^2 \rangle}{V_A^2} = \frac{\langle \Delta B_t^2 \rangle}{B_o^2}, \tag{8}$$

where $V_A \equiv B_o/\sqrt{4\pi\rho}$ is the Alfven speed for the mean field. Now, for a small amplitude fluctuation ΔB at any point, the angle θ between the actual field and the mean field is

$$\theta \approx \Delta B / B_o. \tag{9}$$

Using eq. (9) in eq. (8) and rearranging gives the relationship between the one dimensional velocity dispersion $\langle \Delta V^2 \rangle^{1/2}$, dispersion in field position angle $\langle \theta^2 \rangle^{1/2}$,

Zweibel 1996, in "Polarimetry of the Interstellar Medium, p 486

IRREGULAR MAGNETIC FIELDS AND THE FAR-INFRARED POLARIMETRY OF DUST EMISSION FROM INTERSTELLAR CLOUDS

DMITRI S. WIEBE[1] AND WILLIAM D. WATSON
Department of Physics, University of Illinois, 1110 West Green Street, Urbana, IL 61801; dwiebe@inasan.ru, w-watson@uiuc.edu
Received 2004 May 21; accepted 2004 July 6

ABSTRACT

The polarized thermal radiation at far-infrared and submillimeter wavelengths from dust grains in interstellar clouds with irregular magnetic fields is simulated. The goal is to determine to what degree irregularity in the magnetic fields can be consistent with the observation that the maps of the polarization vectors are relatively ordered. Detailed calculations are performed for the reduction in the fractional polarization and the dispersion in position angles as a function of the ratio of the irregular to the uniform magnetic field and as a function of the relevant dimensions measured in correlation lengths of the field. We show that the polarization properties of quiescent clouds and of star-forming regions are consistent with Kolmogorov-like turbulent magnetic fields that are comparable in magnitude to the uniform cor than the correlation length, L_{corr}, of the fields, the value when the number of correlation lengths, N_{corr}, the dispersion in the position angles, σ_α, finite size of a telescope beam is taken into acc lengths (smaller N_{corr}) because of averaging ove observational data. The smoothing of the polariz cloud and the finite size of the beam can be des number of correlation lengths. In addition, we linear polarization percentage with increasing ir lengths in many, although not all, dark clouds (cutoff in the polarizing effect of dust, thermalizat magnetic field are considered.

Subject headings: dust, extinction — ISM: clou turbulence

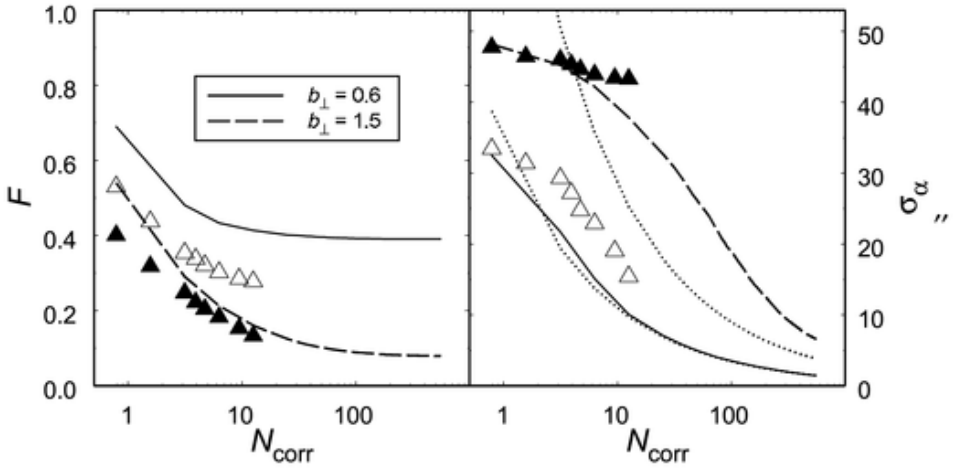

FIG. 1.—Polarization reduction factor F due to turbulence and the dispersion σ_α in the position angle vs. the number of correlation lengths N_{corr} through a cloud. Results from the actual MHD computations are denoted by filled ($b_\perp = 1.5$) and open ($b_\perp = 0.6$) triangles. The dispersion of position angles obtained with the expression of Myers & Goodman (1991) is indicated by the dotted lines.

CHANDRASEKHAR/FERMI vs. ZEEMAN SPLITTING:

C/F gives Bperp, Zeeman gives Blos

WHY DOES C/F "ALWAYS" PROVIDE LARGER FIELDS THAN ZEEMAN SPLITTING?

C/F vs. Zeeman: three reasons...

1. **C/F responds to Bperp, Zeeman to Bpar.**
2. **The Probability Density Functions (PDFs) show that Bpar tends to be smaller than Bperp.**
3. **2. C/F averages over elements along the line of sight, making polarization look more aligned than it really is and making the inferred field strength too large.**
4. **In an expanding shell, systematic motions govern and stretch B to make it more aligned and the inferred field strength too large.**

Reason 1: Bpar tends to be smaller than Bperp...

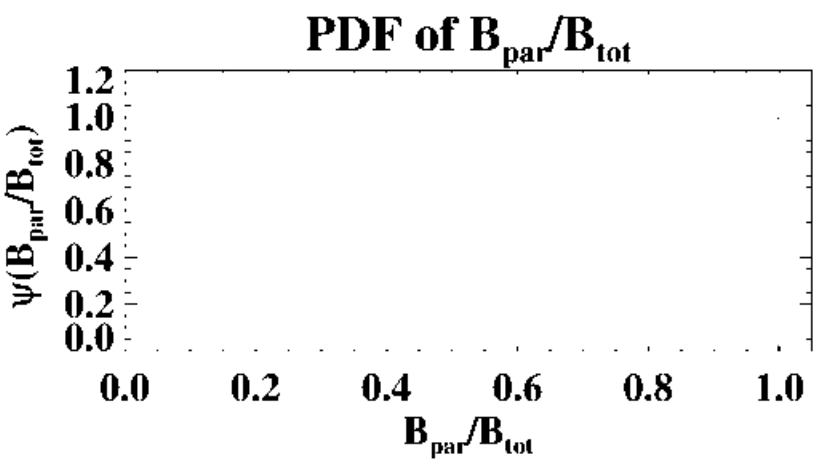
PDF of B_{par}/B_{tot}
$\psi(B_{par}/B_{tot})$
B_{par}/B_{tot}

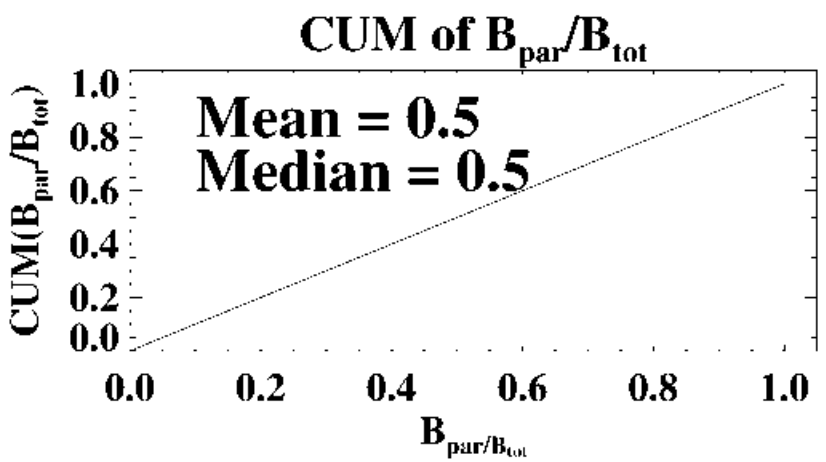
CUM of B_{par}/B_{tot}
Mean = 0.5
Median = 0.5
$CUM(B_{par}/B_{tot})$
$B_{par/B_{tot}}$

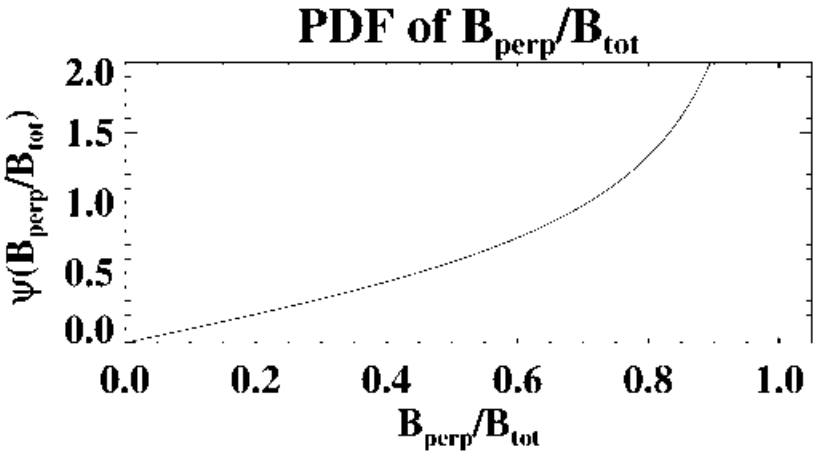
PDF of B_{perp}/B_{tot}
$\psi(B_{perp}/B_{tot})$
B_{perp}/B_{tot}

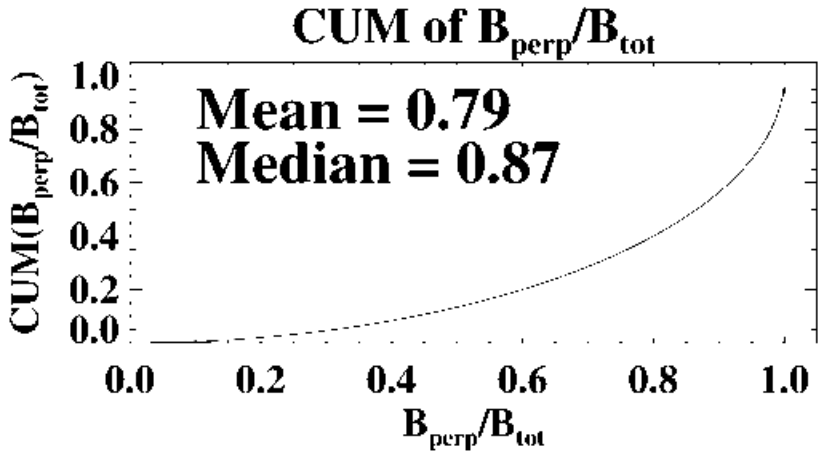
CUM of B_{perp}/B_{tot}
Mean = 0.79
Median = 0.87
$CUM(B_{perp}/B_{tot})$
B_{perp}/B_{tot}

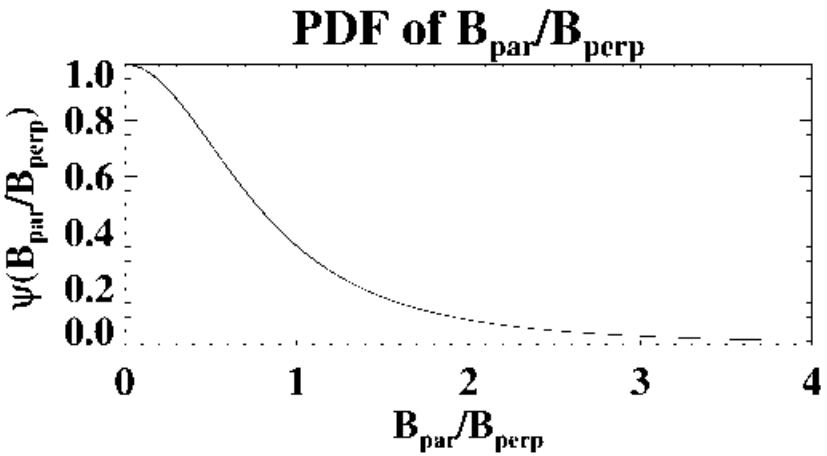
PDF of B_{par}/B_{perp}
$\psi(B_{par}/B_{perp})$
B_{par}/B_{perp}

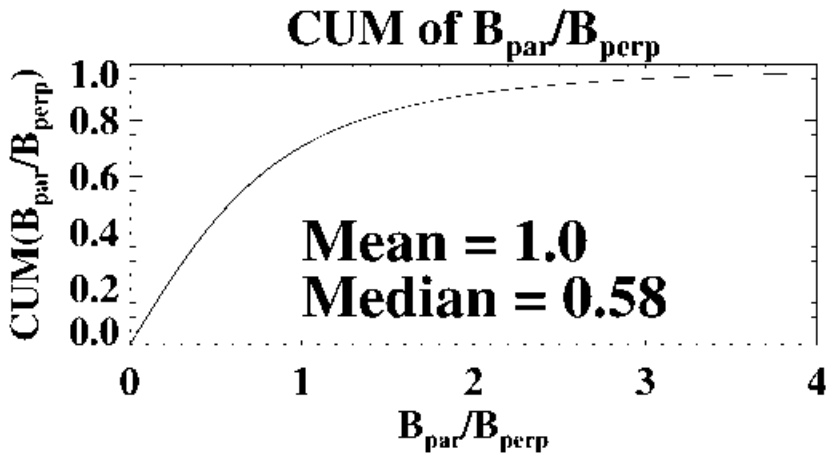
CUM of B_{par}/B_{perp}
Mean = 1.0
Median = 0.58
$CUM(B_{par}/B_{perp})$
B_{par}/B_{perp}

Reason 2: Stellar polarization averages over the line of sight, making the alignment look better than it really is.

The best approach: compare data to numerical models and theory that predict this effect.

The Astrophysical Journal, 695:1362–1369, 2009 April 20 doi:10.1088/0004-637X/695/2/1362

DISPERSION OF OBSERVED POSITION ANGLES OF SUBMILLIMETER POLARIZATION IN MOLECULAR CLOUDS

G. Novak[1], J. L. Dotson[2], and H. Li[3]
[1] Department of Physics and Astronomy, Northwestern University, Evanston, IL 60208, USA; g-novak@northwestern.edu
[2] NASA/Ames Research Center, MS 245-6, Moffett Field, CA 94035, USA
[3] Harvard-Smithsonian Center for Astrophysics, Cambridge, MA 02138, USA
Received 2007 July 18; accepted 2009 January 29; published 2009 April 7

ABSTRACT

One can estimate the characteristic magnetic field strength in Giant Molecular Clouds (GMCs) by comparing submillimeter polarimetric observations of these sources with simulated polarization maps developed using a range of different values for the assumed field strength. The point of comparison is the degree of order in the distribution of polarization position angles. In a recent paper by H. Li and collaborators, such a comparison was carried out using SPARO observations of two GMCs, and employing simulations by E. Ostriker and collaborators. Here, we re-examine this same question, using the same data set and the same simulations, but using an approach that differs in several respects. The most important difference is that we incorporate new, higher angular resolution observations for one of the clouds, obtained using the Hertz polarimeter. We conclude that the agreement between observations and simulations is best when the total magnetic energy (including both uniform and fluctuating field components) is at least as large as the turbulent kinetic energy.

The combination of exquisitely good data and comparison with theory/models says: magnetic energy ~ turbulent energy

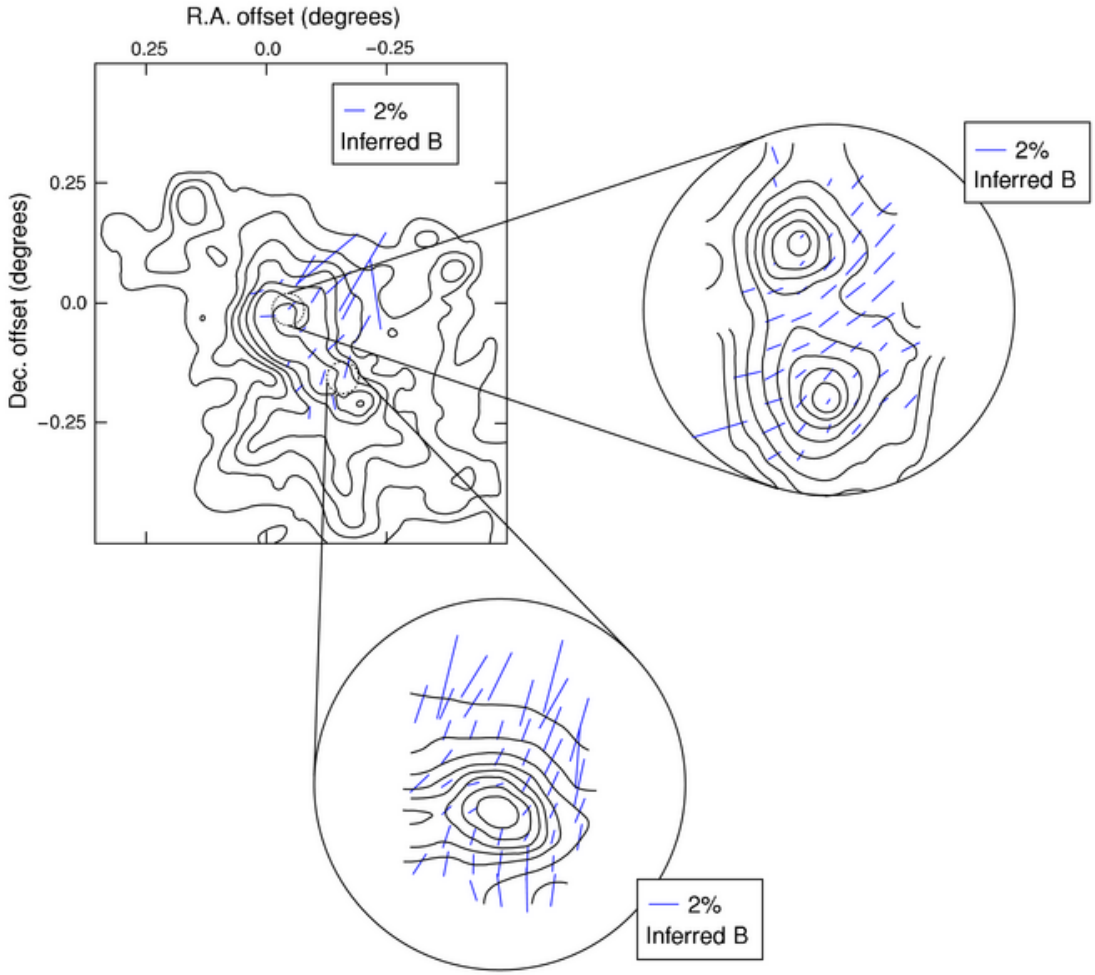

Figure 1. Submillimeter polarimetry of the GMC NGC 6334. The map at upper left (from Li2006) shows 450 μm polarization measurements obtained using SPARO, superposed on 100 μm intensity contours from IRAS ISSA. For two smaller regions within this map (dashed circles), we show expanded views at right and bottom. These "blow-ups" show new 350 μm polarization measurements obtained using the Hertz instrument. The contours in the blow-ups show the 350 μm total intensity, as measured by Hertz. For both SPARO and Hertz results, the direction of each bar indicates the inferred magnetic field direction (which is perpendicular to the measured polarization angle) and the length of the bar is proportional to the degree of polarization. Each polarization map has a key showing the bar length corresponding to a polarization magnitude of 2.0%. The SPARO map is referenced to the following equatorial (J2000) coordinates: ($17^{\rm h}20^{\rm m}51\overset{\rm s}{.}0$, $-35^\circ45'26''$). Each of the two Hertz intensity maps has contours drawn at 20%, 30%, 40%,..., 90% of the respective peak flux.

(A color version of this figure is available in the online journal.)

Reason 3: The ISM is buffeted by shocks—e.g., expanding supershells—which stretches the field and creates alignment that is unrelated to turbulence.

MAGNETICALLY DOMINATED STRANDS OF COLD HYDROGEN IN THE RIEGEL-CRUTCHER CLOUD

N. M. McClure-Griffiths,[1] J. M. Dickey,[2] B. M. Gaensler,[3,4] A. J. Green,[5] and Marijke Haverkorn[6,7]

Received 2006 June 13; accepted 2006 August 26

ABSTRACT

We present new high-resolution (100″) neutral hydrogen (H I) self-absorption images of the Riegel-Crutcher cloud obtained with the Australia Telescope Compact Array and the Parkes Radio Telescope. The Riegel-Crutcher cloud lies in the direction of the Galactic center at a distance of 125 ± 25 pc. Our observations resolve the very large, nearby sheet of cold hydrogen into a spectacular network of dozens of hairlike filaments. Individual filaments are remarkably elongated, being up to 17 pc long with widths of less than ~0.1 pc. The strands are reasonably cold, with spin temperatures of ~40 K and in many places appearing to have optical depths larger than 1. Comparing the H I images with observations of stellar polarization, we show that the filaments are very well aligned with the ambient magnetic field. We argue that the structure of the cloud has been determined by its magnetic field. In order for the cloud to be magnetically dominated the magnetic field strength must be ≥30 μG.

Subject headings: ISM: atoms ISM: clouds ISM: magnetic fields ISM: structure radio lines: ISM

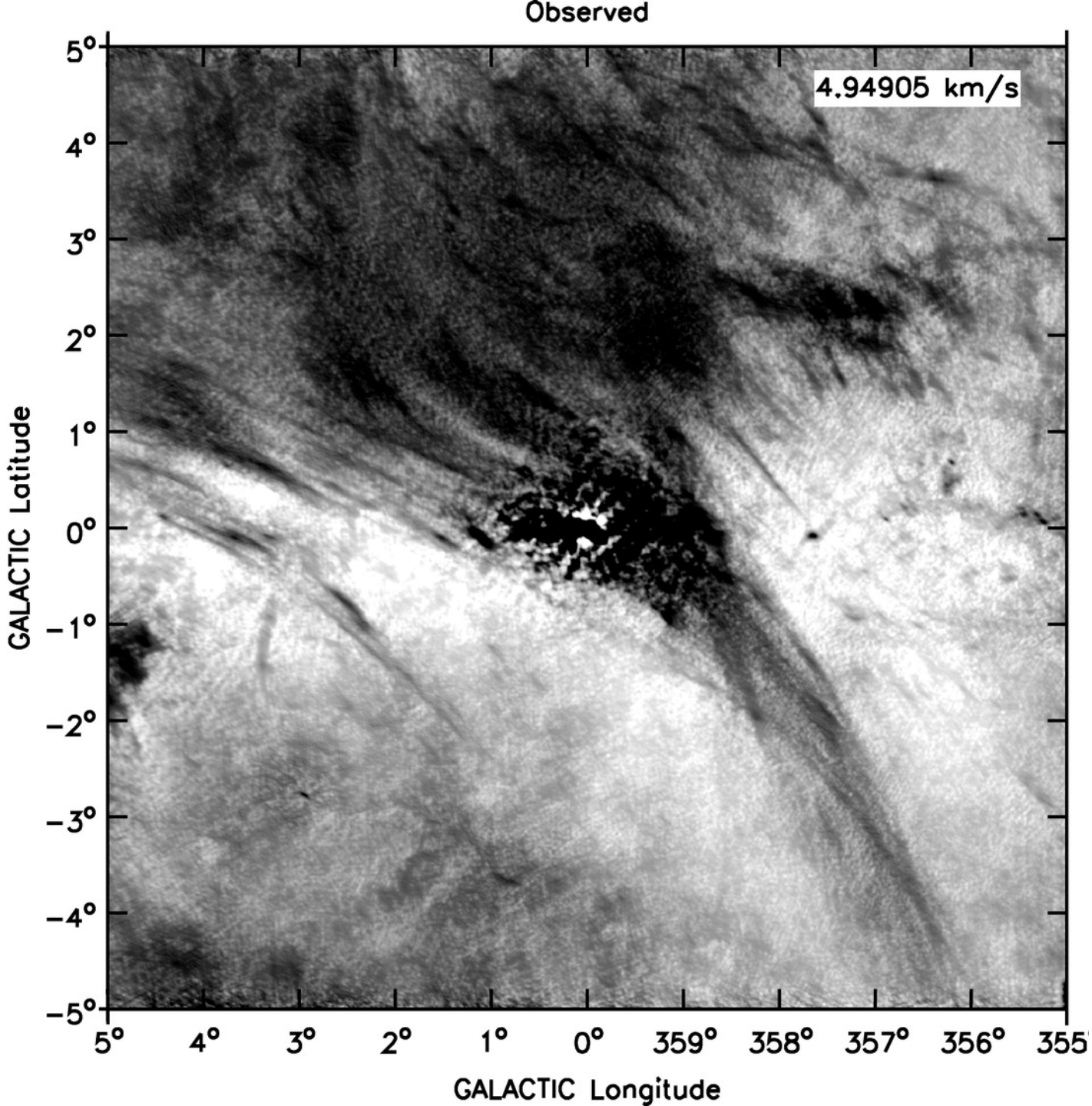
Observed
4.94905 km/s
GALACTIC Latitude
GALACTIC Longitude
5°
4°
3°
2°
1°
0°
−1°
−2°
−3°
−4°
−5°
5°
4°
3°
2°
1°
0°
359°
358°
357°
356°
355

C/F method:

$$\langle B \rangle^2 = \xi 4\pi\rho \frac{\sigma_v^2}{\sigma(\tan \delta_p)^2},$$

gives 60 μG.

But this is part of the NPS—a superbubble expanding at about 20 km/s. Field lines swept up and stretched...

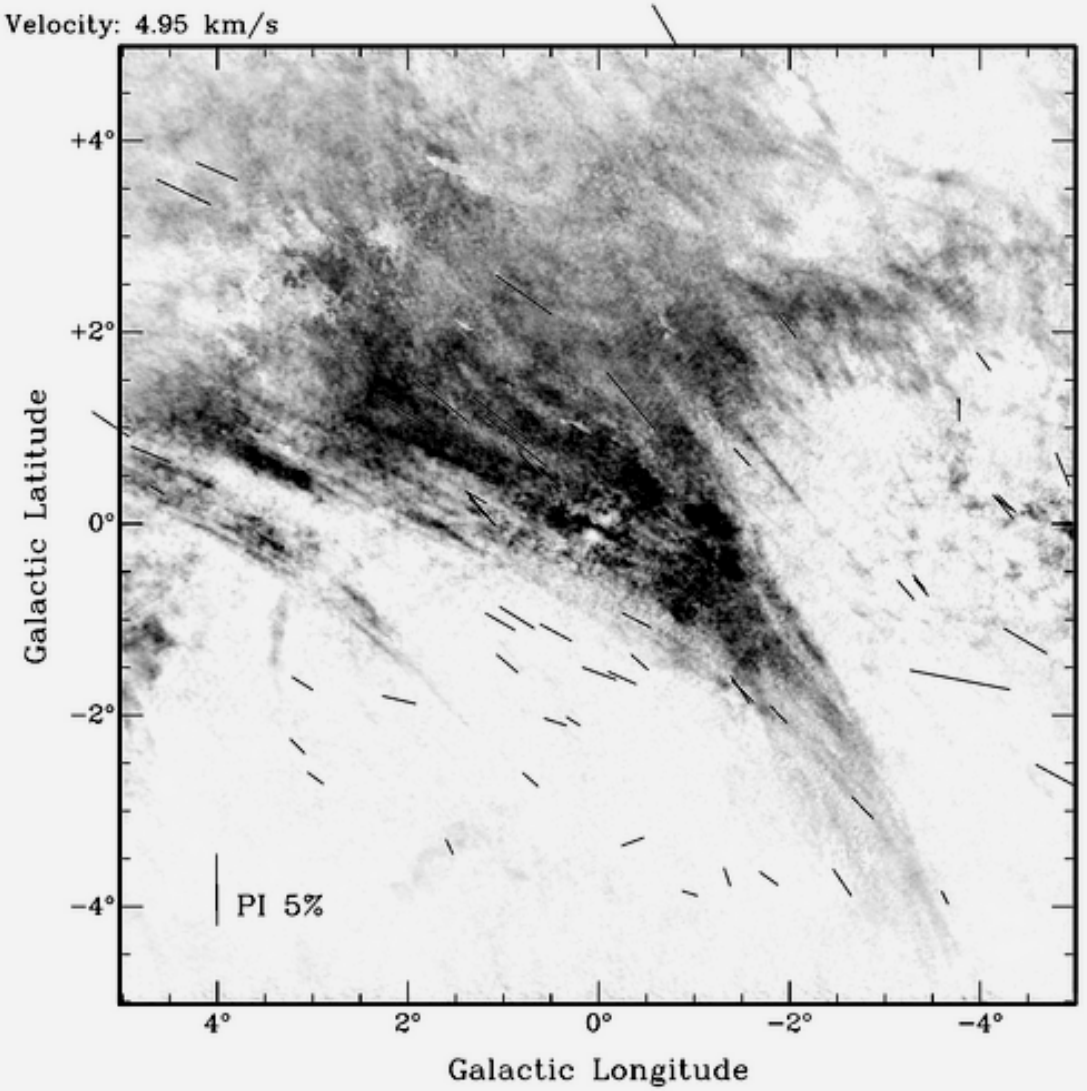

FIG. 6.—H I image of the R-C cloud at $v = 4.95$ km s^{-1} overlaid with vectors of stellar polarization from Heiles (2000). The measured polarization vectors are aligned with the magnetic field direction. The length of the vectors is proportional to the measured fractional polarized intensity, with the scale given by the 5% fractional polarized intensity vector shown by the scale of the vector in the bottom left corner.

Btot:

Synchrotron emissivity

5. SYNCHROTRON EMISSIVITY GIVES THE TOTAL FIELD

5.1. If the relativistic electron spectrum is KNOWN

Relativistic electrons typically have a power law spectrum

$$n(E)\, dE = \mathbf{K_E} E^{-\gamma}\, dE$$

Here $\mathbf{K_E}$ describes the volume density of relativistic electrons. The synchrotron volume emissivity is

$$\epsilon(\nu) = \mathbf{K}_\epsilon B^{\frac{\gamma+1}{2}} \nu^{-\frac{\gamma-1}{2}} \quad (1)$$

Adopt the typical $\gamma = 2.5$ for convenience and combine the above

$$\epsilon(\nu) \propto \mathbf{K_E} B^{1.75} \nu^{-0.75} \quad (2)$$

Near the Sun we supposedly know $\mathbf{K_E}$, and from the measured (Beurman et al. 1985) $\epsilon(408\ \mathrm{MHz}) = 7.3\ \mathrm{K\ kpc^{-1}}$ we infer

$$\langle B^{1.75} \rangle^{\frac{1}{1.75}} \approx 5\ \ \mu\mathrm{G}$$

with $\pm \sim 1\ \mu$G depending on being in a spiral arm or not.

5.2. If the relativistic electron spectrum is UNKNOWN

Here we use the "minimum energy" argument, or the slightly different "equipartition" argument. The electron energy density is

$$W_e = \int_{E_{low}}^{E_{high}} n(E)\ E\ dE \approx \frac{\mathbf{K_E} E_{low}^{-\gamma+2}}{-\gamma+2}$$

The low-energy cutoff E_{low} leads to a low-frequency break in the synchrotron power-law spectrum at

$$\nu_{low} \approx \left(\frac{E_{low}}{m_e c^2}\right)^2 \nu_{ct} \propto E_{low}^2 B$$

where $\nu_{ct} = \frac{eB}{m_e c}$ is the cyclotron frequency. Substitute (1) above to get

$$W_e \propto \epsilon(\nu) B^{-3/2} \nu_{low}^{-\frac{\gamma+2}{2}}$$

Now, for minimum energy, minimize the sum (where $W_B = \frac{B^2}{8\pi}$)

$$W_{tot} = W_e \left(\frac{W_{cr}}{W_e} \right) + W_B$$

NOTE the factor $\left(\frac{W_{cr}}{W_e}\right)$. The Lion's share of the relativistic particle energy is in the **PROTONS!** Near the Sun, $\left(\frac{W_{cr}}{W_e}\right) \sim 100$. Elsewhere people adopt this same ratio. Theorists assure me that this has a rational basis (but I don't know what it is).

We end up with

$$B_{W_{tot},min} \propto \epsilon(\nu)^{2/7}$$

Along a line of sight where $\epsilon(\nu)$ fluctuates, we observe the sum $\int \epsilon(\nu)\, dl$, not $\int \epsilon(\nu)^{2/7}\, dl$, so that $\mathbf{B}_{W_{tot},min}$ **is heavily weighted toward high-field regions**:

$$B_{W_{tot},min} \propto \langle B^{7/2} \rangle^{2/7}$$

Btot:

Ambipolar diffusion

Martin Houde seems to be directly detecting ambipolar diffusion....

HCO^+ vs. HCN and $H^{13}CO^+$ vs. $H^{13}CN$

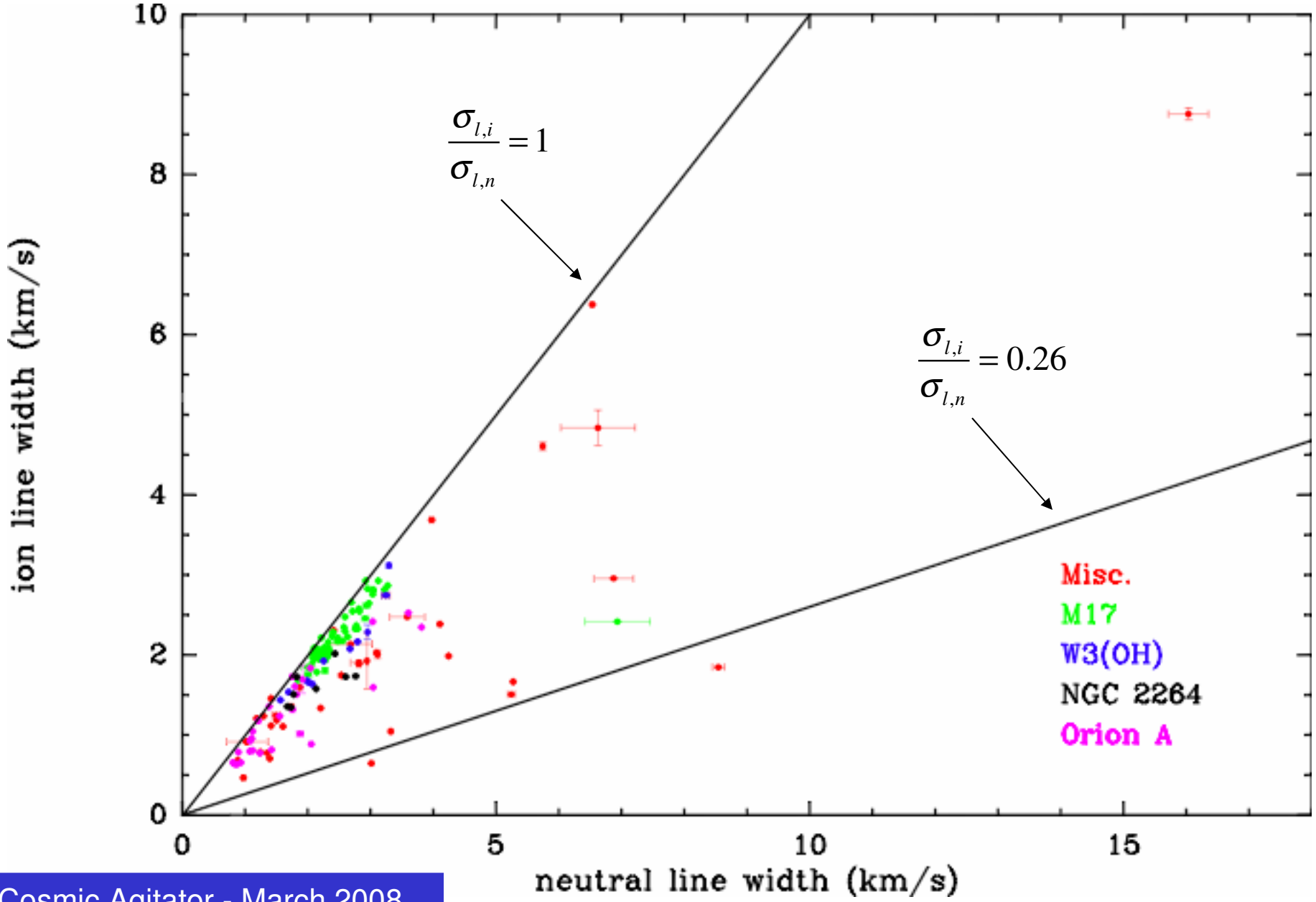

A Study of HCN and HCO^+ in M17

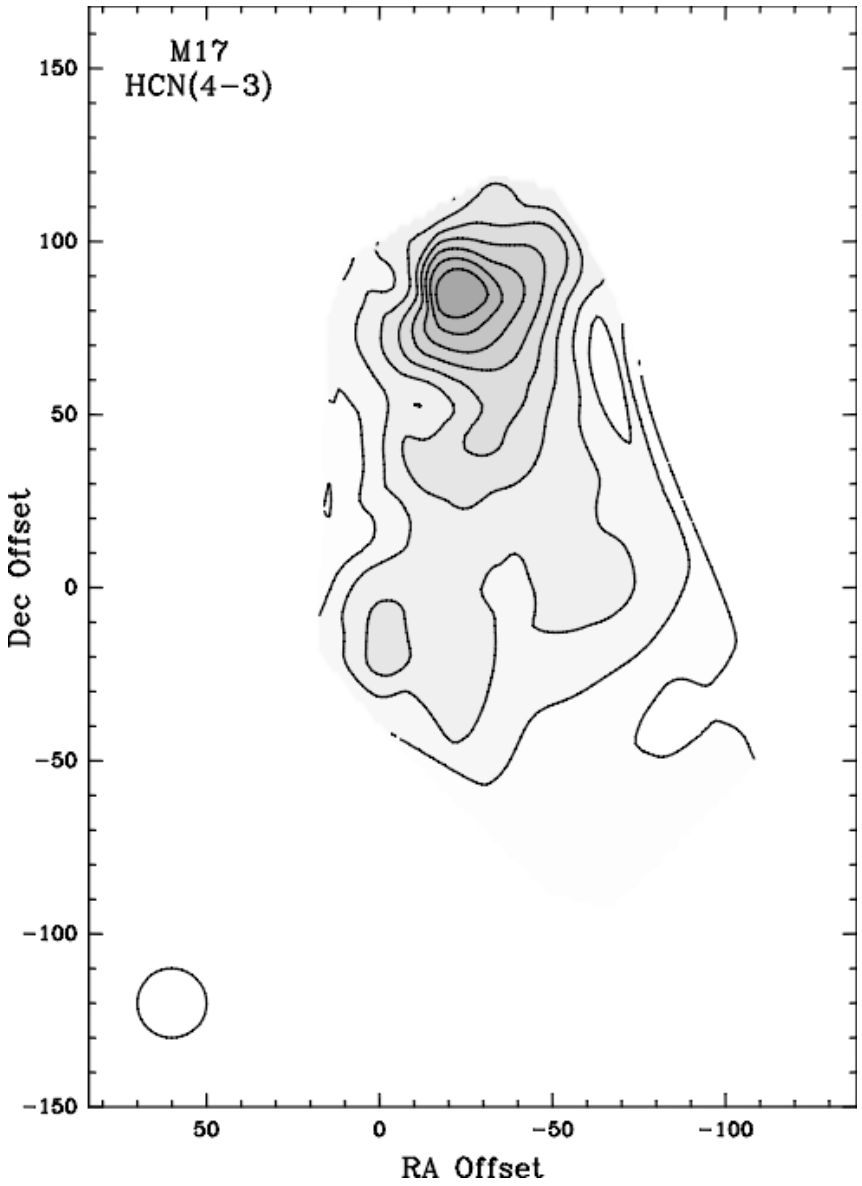

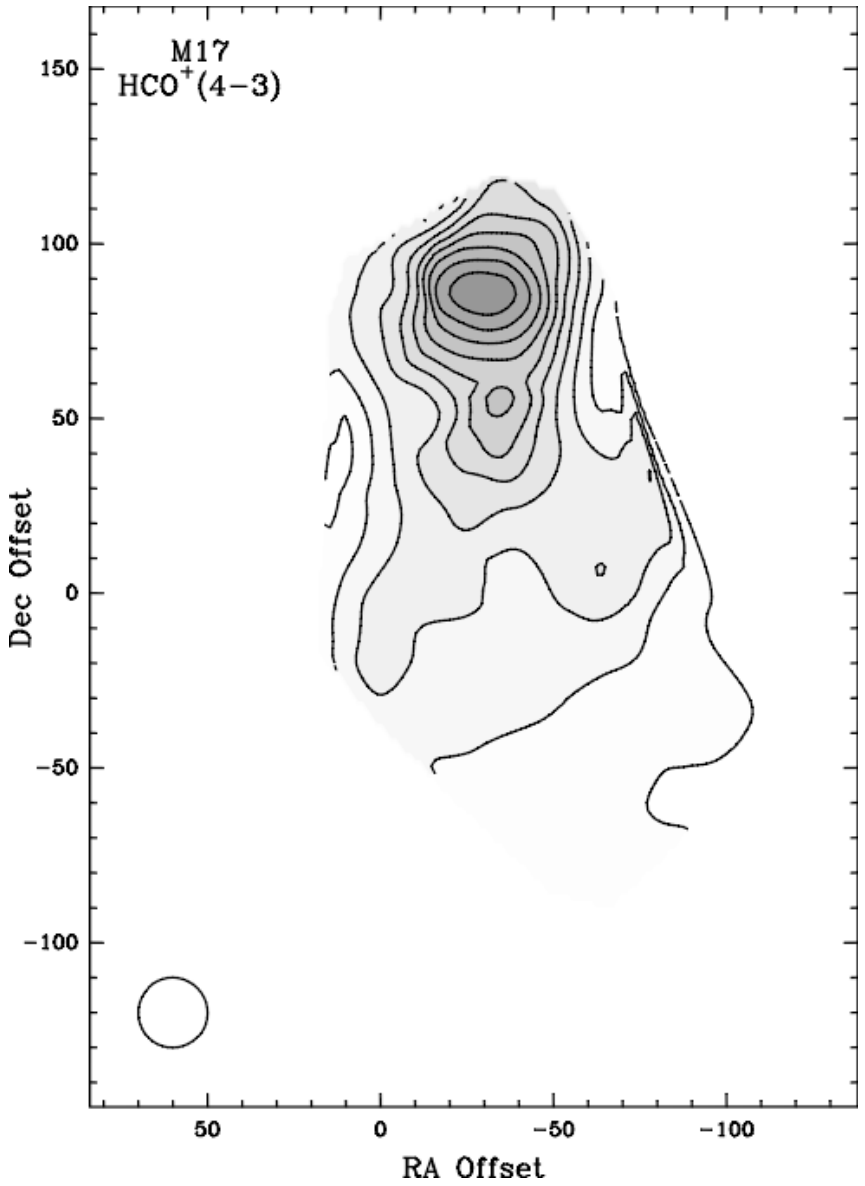

Houde et al. (2002)

Examples of spectra of HCN and HCO^+

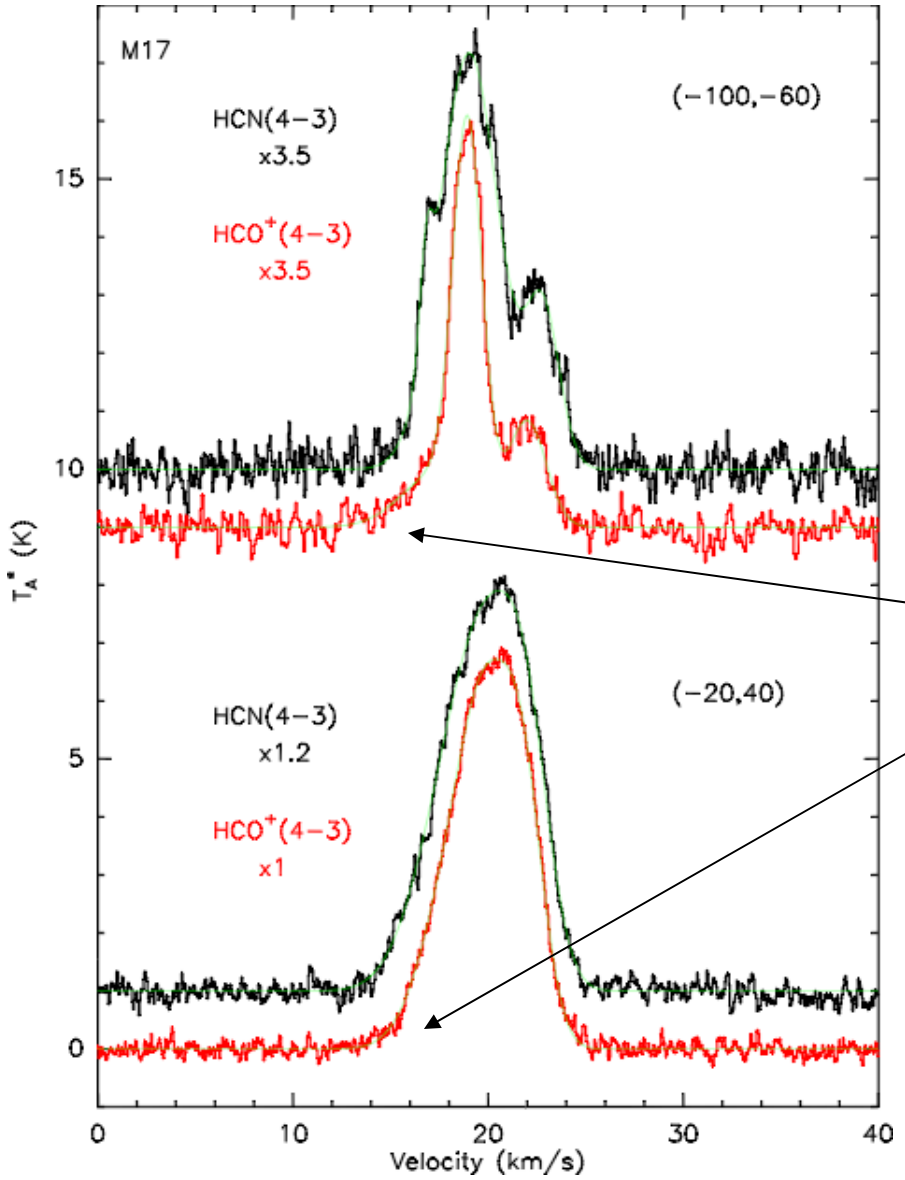

We need a high SNR in order to detect and fit the high(ier) velocity wings...

The magnetic field strength (plane of the sky)

Ambipolar diffusion roughly sets in when the two terms of Ohm's Law are equal

$$R_{\rm m} \equiv \frac{\left|\mathbf{v}_{\rm n} \times \mathbf{B}\right|}{\left|\beta(\nabla \times \mathbf{B})_{\perp}\right|} = \frac{4\pi n_{\rm i} \mu \nu_{\rm i} V_{\rm n} L}{B^2} \approx 1,$$

where $V_{\rm n}$ and L are as defined previously.

The magnetic field strength (plane of the sky)

Transforming this equation...

$$B = \left(\frac{L}{0.5 \text{ mpc}} \right)^{1/2} \left(\frac{V_\text{n}}{1 \text{ km s}^{-1}} \right)^{1/2} \left(\frac{n_\text{n}}{10^6 \text{ cm}^{-3}} \right) \left(\frac{\chi_\text{i}}{10^{-7}} \right)^{1/2} \text{ mG},$$

where χ_i is the ionization fraction.

With $L = 1.8$ mpc and $V_\text{n} = 0.3$ km s^{-1}

B ; 0.3 mG.

The magnetic field strength (plane of the sky)

From wave damping due to ion-neutral friction

(e.g., Kulsrud and Pearce (1969))

$$B = \frac{1}{\pi}\left(4\pi\mu n_{\rm n}\right)^{1/2} \chi_{\rm i} v_{\rm i} L$$

$$= \left(\frac{n_{\rm n}}{10^{6}\ {\rm cm}^{-3}}\right)^{3/2} \left(\frac{\chi_{\rm i}}{10^{-8}}\right)\left(\frac{L}{10\ {\rm mpc}}\right)\ {\rm mG}.$$

With $L = 1.8$ mpc and $\chi_{\rm i} = 10^{-8}$

$$B = \ 0.18\ {\rm mG}.$$

6. OVERVIEW

6.1. Two methods to measure $B_{||}$

- Zeeman Splitting. Gives $B_{||}$ in neutral atomic HI gas.
- Faraday rotation. Gives $B_{||}$ in ionized gas.

These two don't necessarily agree. Towards the Crab Pulsar, Faraday rotation gives $+0.9$ μG and Zeeman splitting gives -3.5 μG.

6.2. Five methods for $B_{\perp}$

- Synchrotron emission. Gives $\langle B^{1.75} \rangle^{1/1.75}$ (where B is the *total* field) and the orientation of $B_{\perp}$ weighted by relativistic electron energy density.
- Polarization of starlight gives the orientation of $B_{\perp}$ weighted by local volume density, usually in diffuse regions.
- Polarization of grain IR emission gives the orientation of $B_{\perp}$ weighted by local volume density, usually in dense molecular regions.
- The C-F method gives the strength of $B_{\perp}$ weighted by local volume density
- The Goldreich-Kylafis mechanism gives ambiguous information on the orientation of $B_{\perp}$, usually in molecular regions.

Fin